Time-Dependent Fracturing in Rocks to Tackle Tight Geothermal Reservoirs in the Netherlands

by

Emilio Cecchetti

Supervisors:

Dr. Jan Ter Heege (TNO)

Dr. Fred Beekman (UU)

Utrecht University

TNO innovation for life

Abstract

Tight geothermal reservoirs represent large sources of energy which could significantly help to meet the rising demand in clean energy. However, the extremely low hydraulic conductivity within these reservoirs hampers the flow between injection and production wells, making the economic success of the operations dependent on the application of a series of stimulation treatments. Conventional stimulation methods are sometimes associated with drawbacks as induced seismicity and environmental hazards. In this study, I have introduced and tested the concept of time-dependent (subcritical) fracturing to enhance reservoir permeability. This process implies the occurrence and growth of fractures under loads that are insufficient to cause instantaneous breakage of the rock. The occurrence of subcritical growth of fractures in tight rocks has been tested using a numerical approach, by integrating such a process in existing geomechanical codes (FLAC3D). With the built-in programming language "FISH", I implemented my constitutive model tailored at mechanical and flow behavior, and with the equations derived from Atkinson (1982) and Zurkhov (1984). I first tested out the theory on a small model, simulating the injections in a tight sandstone core sample. Afterwards I applied the method to perform a qualitative analysis at reservoir scale, representing a typical geothermal doublet system, using the software developed by TNO "DoubletCalc" as benchmarking tool for pressure field development. These series of simulations allowed to explore the occurrence of time-dependent fracturing as result of low rate fluid injections, and the effect of such a process on enhancing reservoir permeability. Additionally, the conditions favorable for the initiation of subcritical growth of fractures have been analyzed in relation to the lifetime of a geothermal doublet system.

Table of Contents

List of Figures

List of Tables

1. Introduction

Nowadays energy supply and use are largely based on fossil fuels and therefore unsustainable. Energy-related emission of CO_2 is expected to double by 2050 if preventive measures are not adopted. Geothermal energy represents a sustainable and reliable source of energy, even if its application is limited to areas where geological conditions allow fluids to transfer heat from the Earth's interior to the surface through high temperature wells. Geothermal resources at relatively low temperatures can be found in many aquifers and be exploited through binary power plants, combined heat and power plants or in heat-only applications (Technology Roadmap, 2011). To speed up this energy-transition process and meet the rising global demands for energy, the geothermal industry is continuously seeking for new methods to enlarge and optimize energy production.

In geothermal operations, beside the temperature, an important parameter which determines the success of the operations is the fluid flow rate. In areas with low geothermal gradients such as the Netherlands, the high temperatures (>100°C) are found deep (> 3 km) below the surface, where reservoirs are generally too tight to be exploited without stimulation of flow. These deep resources are extensive and can significantly contribute to a more sustainable energy production. However, the low permeability (< 1 mD) and porosity (< 10%) of many deep and tight reservoirs hampers high flow rates between the injection and producer well, thereby minimizing the heat production of the system. Especially in sedimentary reservoirs, low permeability and porosity are usually related to different diagenetic processes including mechanical compaction, chemical solution and cementation (Marfil et al., 1996). For these reservoirs, the economic success of the operations is dependent on the application of (a series of) stimulation treatments to the reservoir. These operations generally consist of opening existing fractures or creating new ones, and require methods to keep fracture networks open to reduce the flow limiting problems and maximize heat production (Portier et al., 2009). Stimulation methods are sometimes associated with the occurrence of induced seismic events and environmental hazards such as pollution. Therefore, preventive measurements and different approaches need to be tested to minimize these risks.

The main purpose of this work is to evaluate existing stimulation approaches and associated drawbacks, together with introducing and testing the concept of time-dependent (subcritical) fracturing as result of low rate fluid injections to enhance permeability in tight reservoirs. To properly describe this concept a coupled and flow approach is required, i.e. the rise in pressure due to fluid injection causes fracture deformation, which, consequently, enhance the permeability and the injectivity rate. To simulate this process, I have used FLAC3D (Fast Lagrangian Analysis of Continua in 3 Dimensions), a software developed for mechanical simulations that include possibilities to simulate coupled mechanical and flow processes. In particular, these simulations have been carried out below the fracturing pressure, which implies injecting lower volume of fluid over time in comparison to the conventional hydraulic fracturing treatments. These series of simulations would allow to understand better how low rate fluid injections affect effective stresses and poroelastic deformation. Furthermore, the retrieved effective stress values will be used to implement the equations proposed by Atkinson (1982) and Zurkhov (1984) in the model, which express the basis of the time-dependent fracturing approach. The results will be then evaluated to assess the effects of the process on hydraulic conductivity enhancement over time. The success of this process could improve reservoir quality without significant overpressure occurrence, constraining the risks associated with conventional stimulation jobs.

Overall, simulations show that time-dependent fracturing occur as result of fluid injections below the fracturing pressure. Such a process can affect permeability over time. Furthermore, favorable

conditions for initiation of subcritical fracturing has been observed to be reached below values of pressure required to create conventional fractures, even during simple fluid circulation in a geothermal doublet system.

2. The Trias Westland Geothermal Project

Although low permeable and porous reservoirs have generally been considered to be unfavorable for geothermal exploitation, the increasing demand in sustainable heat sources has caused operators to start considering these tight reservoirs for future geothermal operations. In the Netherlands, one of the most investigated and promising tight reservoirs is a Triassic sandstone formation, part of the Lower Germanic Trias Group, located in the Westland Municipality (figure 1). This reservoir is potentially able to provide heat covering about 80% of the heat demand in the Westland area. This estimate is partly due to the relatively high temperature water estimated to range between 130 and 150 °C (www.ta.survey.nl).

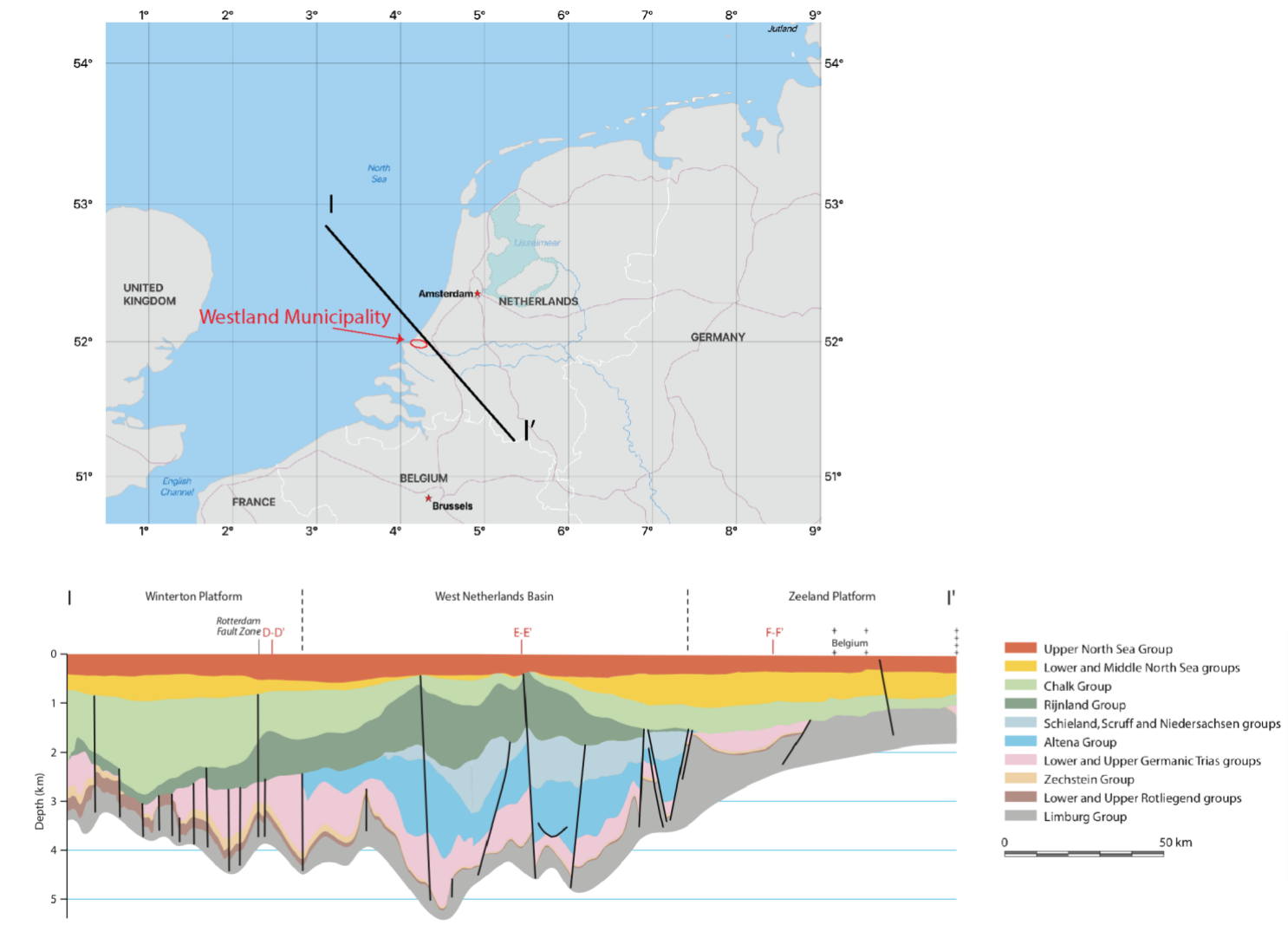

Figure 1: Location of the Westland municipality in the South-West part of the Netherlands and cross section showing the Lower and Upper Germanic Trias Groups containing the investigated Triassic sandstone formation.

In 2017, the first drilling test was performed as part of Trias Westland Geothermal energy project. The cores samples obtained during drilling operations were then analyzed and tested to retrieve reservoir petrophysical properties. Porosity and permeability of the samples were assessed by direct measurements of grain volume and bulk volume, and through a nitrogen permeameter respectively (Felder et al., 2018). Preliminary results for horizontal plug samples, from depths ranging between 4249 and 4280 m, show a helium porosity values range from 1.4% to 3.9% and Klinkenberg permeability values range from 0.00 to 0.02 mD (figure 1). After a series of core sample analysis and other careful evaluations of the reservoir properties, it was concluded that the Triassic formation is not suitable for cost-effective heat recovery without hydraulic fracturing. Hence the operations in the Triassic reservoir were stopped and the overlying Lower Cretaceous formation, part of the Schieland, Scruff and Niedersachesen Groups (figure 1), located at a depth of 2.7 kilometers became the mean target for heat recovery in that area (www.ta.survey.nl).

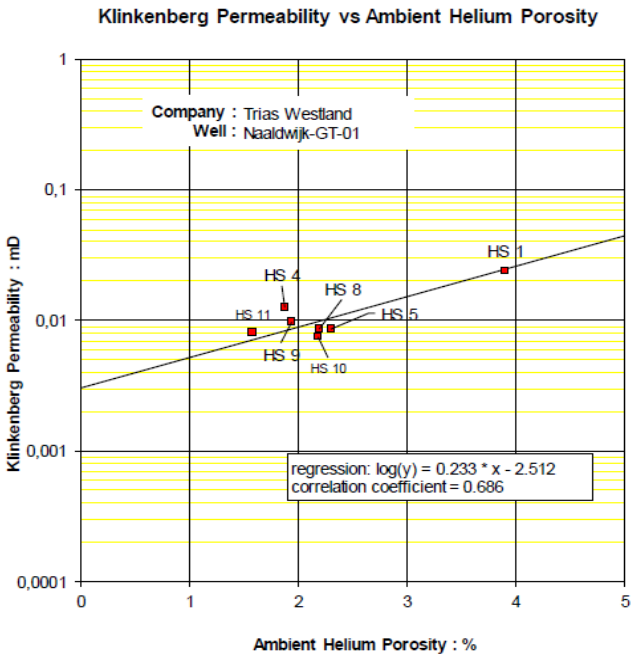

Figure 2: Ambient Porosity vs Klinkenberg Permeability (Felder et al, 2018).

3. Stimulation methods overview

Existing and new geothermal wells can experience dips in injectivity or productivity during operations. An initial good performance can decline over the lifetime of a geothermal project. In some cases, wells drilled in low permeability reservoirs require stimulation treatments at the beginning of operations to obtain required flow rates.

Many stimulation treatments have been developed by the oil & gas industry, ranging from acid treatments to clean pre-existing fractures in the near well area to massive hydraulic fracturing treatments, to create new or extend pre-existing fractures. The occurrence of new fractures is a result of fluid injections above the fracturing pressure: the high-pressure fluid injections cause pressure to raise in area nearby the injection point and, consequently, one or multiple tensile or shear fractures will develop depending on the local stress state and presence of natural faults or fractures (figure 3).

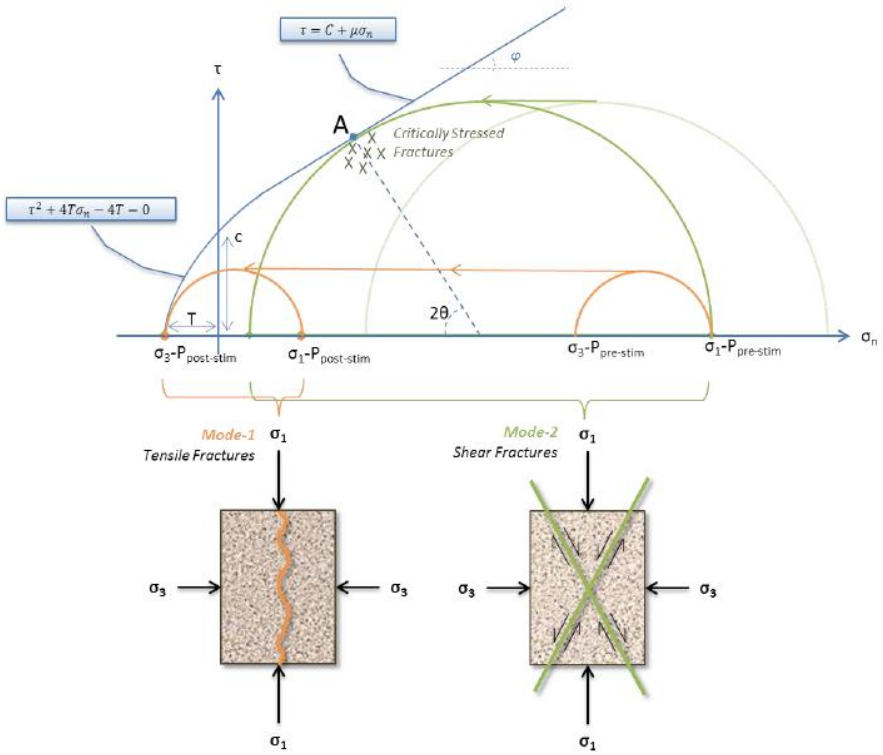

Figure 3: Mohr-Coulomb envelop representing the effect of increasing pore-pressure for two different stress fields. Low differential stress will cause the fracture to be generated in a tensile mode. Conversely for high differential stress the fracture will be generated in shear mode. Picture from TNO 2015 R11618|Final report.

Proper application of such treatments usually significantly contributes to increase well flow rates, increasing the well lifespan and maintaining the high well flow rates over years. The next paragraphs provide an overview about the most commonly used stimulation techniques which are also applicable to the geothermal industry.

3.1 Acid stimulation

Acidizing is one of the oldest stimulation techniques used in the oil & gas industry. This technique has also been adopted by geothermal companies all over the world. Similar to most of the other stimulation techniques, its aim is to increase the formation permeability and porosity in particular near the wellbore to enhance fluid flow (Economides and Nolte 2000; Halliburton 2000a, b). In particular this stimulation process aims to clean-up pre-existing fractures by dissolving and removing filling materials (Portier 2007). This type of treatment has been successfully applied in different geothermal systems, helping to increase the productivity of the system and decrease the formation damage effects (Table 1 and 2).

Geothermal Field	Number of treated wells	Vaariation of the injectivity index before and after the acid treatment (kg/s/bar)	Improvement factor
Bacman (Philippines)	2	0.68 -> 3.01 0.99 -> 1.4	4.4 1.4
Leyte (Philippines)	3	3.01 -> 5.84 0.68 -> 1.77 1.52 -> 10.8	1.9 2.6 7.1
Las Tres Virgenes (Mexico)	2	0.8 -> 2.0 1.2 -> 3.7	2.5 3.1

Table 1: Results of chemical treatments in crystalline reservoirs. Data from Portier et al., 2007.

Wellbore Parameter/ Discharge Test Results	OP-3D		OP-5DA	
	Pre-acid	Post-acid	Pre-acid	Post-acid
Injectivity Index (li/s/Mpa)	6.8	30.1	9.9	14.0
Pressure drop, ΔP (Mpag)		1.2		2.5
kh (darcy-m)	3.22	3.18	3.1	3.2
Skin	+3.2	-5,5	+8.3	-4.7
Discharge WHP (MPaA)	0.7	0.71	0.7	0.7
Power Output (Mwe)	2.7	5.5	1.5	4.1

Table 2: Results of chemical treatments on sandstone reservoir (Philippine). Data from R.C.M Malate et al., 1998.

Over the years, many acids have been tested for different formations and purposes. In 1940, Dowell introduced a mixture of HCl and HF acid to reduce the possibility of reaction products precipitation. The mixture, which is still commonly used especially for sandstone's reservoirs, is often referred to as "Mud Acid". It is made up by a concentration of 3% HF and 12% HCl as described by Smith and Hendrickson (1965) and Abdelmoneim and Nasr-El-Din (2015). Two basic types of acidizing operations can be performed:

1)Matrix acidizing**:** which is executed below fracturing pressure and is generally used to remove the skin damage and increase the formation permeability (S. Portier et al., 2007). In this particular process the used acid flows through the matrix reacting with the rock's particles in the existing pores and fractures.

2)Fracture acidizing**:** where the acid is injected above fracturing pressure, therefore creating new and not just to perform damage removal. This technique is mostly used to create conductive paths further away from the well(fractures and Nolte, 1989).

Acid treatments are mostly used for wells with reduced productivity over time. In fact, the acid can improve the productivity, and thereby the well's lifespan. Before any acid-stimulation, a detailed. evaluation of the formation's property should be carried out, as the success of the treatment mainly depends on the understanding of the chemical and physical reactions between the formation's minerals and the acidizing fluid (Portier, 2007).

3.2 Hydraulic fracturing

Hydraulic fracturing is a technique that can significantly increase production using high permeable fractures that are created by injecting fluids above the fracturing pressure of the formation . In other words, the accessible reservoir area (drainage area) is increased by enlarging the operative wellbore radius. The process involves the high-pressure injection of 'fracturing fluids' primarily composed of water, containing chemical agents and suspended proppants. Some chemicals are used to increase the viscosity (or proppant carrying capacity) of the liquid. Others reduce friction along the wellbore during injection ("friction reducers") or prevent grow of bacteria or algae ("biocides"). The generated fractures will increase in size of number until a drop in pore pressure occurs in the area nearby the

wellbore. This drop in pressure may be due to the increase in permeability or if liquid stops to be pumped into the system. Due to the drop in pressure the induced fracture may close. To avoid low permeability of closed fractures, a propping agent (generally sand particles or ceramic spheres), is added to the fluid and then deposited into the fractures during the stimulation treatment (Economides and Nolte, 2000).

According to Reinicke et al. (2010),three different hydraulic stimulation approaches may be distinguished, depending on the rock, formation and fluid properties:

- Hydraulic proppant fracturing (HPF): Usually, highly viscous gels with high proppant concentrations are used to create highly conductive, but relatively short fractures in a permeable reservoir with a porous matrix. The induced fractures connect the well with the a larger reservoir volume and hence reduce the skin factor (Dake, 1978). After proppant emplacement, the fluid flows from the fracture into the formation ("fluid leakoff") and, consequently, the pressure decreases causing partial closure of the fractures and fixation of the proppant. This treatment is generally used in medium to high permeable formations (10-1000 mD). Proper design of the fracturing treatment allows the induced fractures parameters, for example length, height and conductivity, to be controlled.
- Water fracturing (WF): Water mixed with friction-reducing chemicals (slick water) and low proppant concentration (mainly sand) is pumped into the formation to create long and narrow fractures. The low viscosity of the fluid makes easier to create fractures further away from the injection area and to connect the well with parts located further away into the reservoir, but reduces the carrying capacity of proppants. The main advantage of this technique compared to the HPF is the reduction in cost and less use of fracturing chemicals. Recent studies have shown that this technique is particularly appropriate for reservoirs with permeability lower than 1 mD, where it is important to reactivate existing natural fractures because of the low diffusion of fluid through the rock matrix (Britt et al., 2006; Fredd et al., 2000; Mayerhofer and Meehan, 1998). The success of this technique strongly depends on the ability of the rock to maintain unpropped fracture conductivity. In fact the new open fractures may close as result of creep and pressure solution processes at the asperities (Britt et al., 2006). Injection of propping agents can limit rapid fracture closure while maintaining fracture conductivity, but the proppant carrying capacity of slickwater is low (Fredd et al.,2000). The low viscosity of the injection fluid can lead to unfavorable proppant placement, limiting the fracture length and, consequently, the production potential (Warpinski, 2009).
- Hybrid fracturing: this method is a combination between HPF and WF and aims to combine advantages of WF (large reservoir stimulated volume) with that of HPF (high proppant carrying capacity). Basically, it consists of injecting a slick water to create the fracture geometry and, after that, a gel treatment carries the proppant load to the end of the induced fractures. The geometry of the created fractures is different from the conventional fracking method (HPF) mentioned above: fractures are longer compared to HPF and the effective propped length is higher (Coronado, 2007; Rushing and Sullivan, 2003).

3.3 Risks associated with stimulation operations

Stimulation treatments performances can sometimes have drawbacks such as induced seismicity and environmental pollution. Especially for the case of hydraulic fracturing, one of the most recurrent problem is the occurrence of damaging seismicity during/after the stimulation processes (Kirkman et al., 2017). Most induced seismicity has low magnitudes (micro-seismicity) and is generally harmless and not felt by human beings(SHIP). In fact, especially in tectonically inactive areas, the magnitudes of induced events as a result of hydraulic fracturing treatments are usually below M=1 on the Richter scale(Ellsworth, 2013). However, the occurrence of larger magnitude (up to M 4.6) events have been observed for shale gas hydraulic fracturing in Alberta (Schultz et al., 2018). In fact, in areas with seismic

risk a “traffic light system” can be used to reduce seismic risks, where induced seismicity is constantly monitored. If some critical levels of earthquake magnitude or ground motion are exceeded, operations can be temporarily suspended and the stimulation treatment program properly adjusted or stopped(Mignan et al., 2017).

Environmental pollution also plays a major role in the perception of stimulation treatments. Hydraulic fracturing is generally performed in reservoirs which have no hydrological connection to shallow aquifers or drinkable water. Reservoirs are generally overlain by sealing formations (e.g. claystones, salt layers...) which prevent the exchange of formation fluids with the shallow layers. However, when fracturing treatments are performed, the integrity of top seals or zonal isolation of wells may be jeopardized. These type of risks should be carefully assessed to avoid fluid migration from the target reservoir towards shallow aquifers that may result in environmental pollution. This assessment is of vital importance, since the shallow aquifers may be used as an irrigation or drinking water resource (Vengosh et al.,2014).

Injections of fluids below the fracturing pressures could help mitigate these risks. The lower pressures generated in the reservoir, comparing to the ones generated as result of high rate fluid injections, would decrease the risk of triggering bigger seismic events. Furthermore, because the process would not involve the injection of strong acids into the reservoir, potential migration of fluids towards the surface would not result in environmental pollution in the shallow layers.

4. Static Fatigue and Subcritical crack propagation in rocks

Static fatigue or subcritical crack propagation has been identified as mechanisms that lead to time dependent fracture propagation, resulting into a time dependent reduction of rock strength or relation between time and rock failure stress. Zhurkov (1984) suggested a kinetic theory to explain the process of materials failure. He considers the fracture of solids as a time process dependent on the mechanical stress and the material temperature. He developed a model and evaluated model prediction using tensile tests on fifty different materials . The model leads to the following equation between time to failure (t) and tensile stress (σ):

$$t = t_0 exp\left[\frac{U_0 - \gamma\sigma}{kT}\right] \quad (1)$$

Where t_0 is the reciprocal of the natural oscillation frequency in atoms, U_0 the energy barrier determining the probability of breakage of the bonds responsible for strength, γ is a ratio of bond overstress to average mineral stress, σ is the applied tensile stress, k is the Boltzmann’s constant and T is the absolute temperature. Kear and Bunger (2014) performed flexure tests on crystalline gabbro rocks. These tests, which are well-established methods for estimating the tensile strength using samples of simple geometrical shape, were used to estimate when the failure took place in the point where the maximum tensile stress was induced. Following these authors, Eq. (1) can be simplified (assuming constant temperature) as:

$$t \propto exp\left[\sigma_{tensile}\right] \quad (2)$$

Accordingly to equation 2, a rock will fail at a time that is exponentially proportional to the applied tensile stress. Therefore, even if the applied tensile stress is below the tensile strength for instant loading , the rock will fail over time . This concept also called “delayed fracturing”, referring to the fact that a period of time is required for a fracture to grow large enough to cause tensile failure. This theory has been observed and proven also in porous rocks, as Uwaifo Efosa Christopher (2015) demonstrates through his experiments on critical breakdown pressure on sandstone. Critical

breakdown pressure, corresponds to when hydraulic fracture initiates, is defined as the pressure developed at the wellbore such as the applied stress equals the tensile strength of the rock.

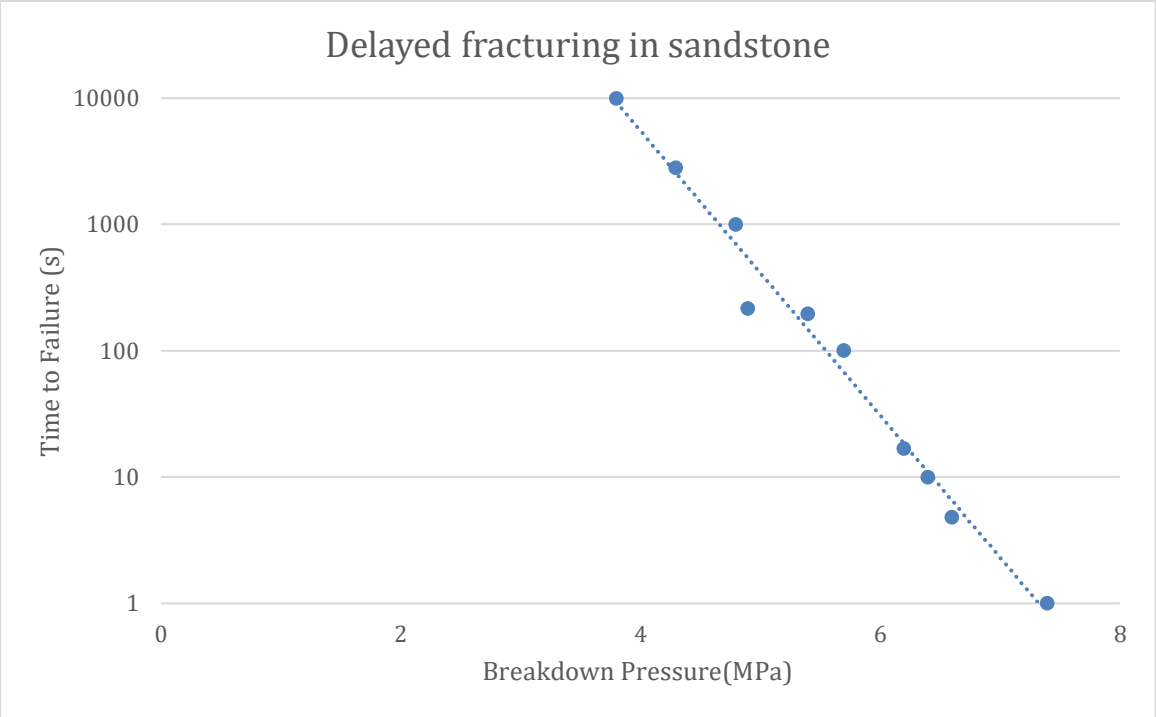

Figure 4 : Relation between time to failure and pressure retrieved from Uwaifo Efosa Christopher (2015) .

Figure 4 describes the relation between the time to failure and breakdown pressure, retrieved from series of experiments on sandstone samples, which confirm the validity of equation 2.

This static fatigue or delayed fracturing process can be observed at microscales and is described by the subcritical crack growth (SCG) theory which explains how fractures propagate at stresses lower than required for slip in any crystallographic system.

Irwin (1957) define three main types of singular stress field and relative crack propagation (figure 5): Mode I (tensile), Mode II (in-planar shear), Mode III (anti-planar shear).

For modeling of fracturing, Mode I is of primary interest as it is the dominant mode for tensile fracturing due to increasing pore fluid pressures. Furthermore, Irwin attributes a fundamental role for the stress intensity factor K_I as a measure of material resistance to fracture. He demonstrated that, for a 2D crack opened by a constant pressure in a tensile mode, the stress intensity factor K_I can be written as:

$$K_I = Y\sigma\sqrt{L} \qquad (3)$$

Where Y is a geometrical constant, σ is the remote applied stress and L is the characteristic half crack length. If the stress intensity factor reached a critical value K_{IC}, typical of the material, the crack will start grow.

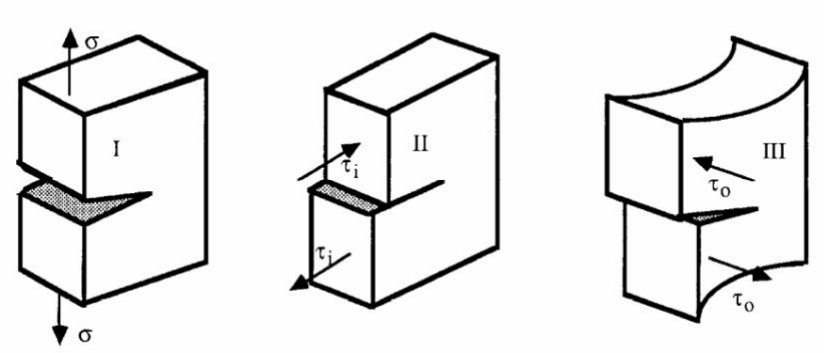

Figure 5: three basic modes of loading for a crack and the relative crack surface movement.

In fracture mechanics studies, it has been demonstrated that a crack in a porous brittle media can propagate at much lower value of K_{IC} (Atkinson, 1982). This subcritical growth can be caused by several competing mechanisms, such as stress corrosion, diffusion, dissolution, ion exchange and microplasticity. A mechanism will be dominant depending on a specific range of environmental and material conditions.

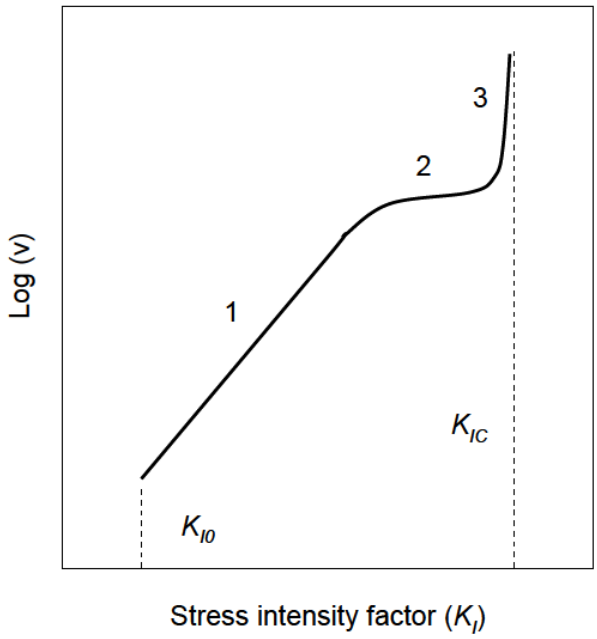

Figure 6: Schematic stress intensity factor (KI) – crack velocity (v) curve. KI0 and KIC represent the threshold and the critical stress intensity value respectively.

As can be seen in figure 6 there are generally three main different regions of behavior defined by K_I thresholds. The behavior in zone 1 is controlled by the rate of stress corrosion reaction at the crack tips. Region 2 is mainly affected by transport of reactive species, however because velocity in this region doesn't change much, it is estimated to be SCG rate controlled. Lastly, region 3 is mainly dominated by mechanical rupture (induced by thermally activated processes). It is assumed that there is a threshold below which no significant crack propagation can occur through stress corrosion (K_{I0}).

The actual time dependency of the crack growth is controlled by processes acting at the tips of cracks where stress concentration exists. The crack propagation velocity can vary as a function of the stress intensity factor (K_I). The Charles's (1958) power law dependence it is most widely used to delineate

the crack growth velocity in the stress corrosion regime (zone 1 in figure 6) for tensional model of deformation at constant temperature. This equation is often presented in literature as follows:

$$v = v_0 e^{(-\frac{H}{RT})} K^n \quad (4)$$

Where *H* is the activation enthalpy, *R* is the gas constant, *T* is the absolute temperature, v_0 is a pre-exponential constant and *n* is a material constant called the stress corrosion index. This formula can be further simplified by assuming a constant temperature. For loading in mode I, the relationship can be expressed as follows:

$$v = AK_1^n = A(\frac{K_I}{K_{IC}})^n \quad (5)$$

Where A and n are the SCG parameters, which can be determined experimentally.

5. Modelling approach

To represent the subcritical crack propagation as result of fluid injections, a model integrating fluid and mechanical analysis is required: fluid flow and the associated pore pressure change causes poroelastic changes in stress. Within this analysis, the associated values of the developed stress field are used to implement the fracturing process in the model and permeability in the model updated accordingly. Temperature is assumed not to change during the simulations, therefore thermoelastic effect is not taken into account. Furthermore, the change in pore pressure generated by the change in fracture volume has not be implemented.

This modelling approach allows to explore the effect of time-dependent (subcritical) fracturing on reservoir permeability. Additionally, pore pressure and stress changes for different injection/depletion rates are modelled for a doublet geothermal system to determine conditions that may favor initiation of subcritical crack propagation.

5.1 Modelling of flow and mechanics

Assuming laminar flow, the basic law governing flow through porous media is the Darcy's law:

$$Q = -\frac{kA}{\mu}\frac{dp}{dr} \quad (6)$$

Where μ is the viscosity of the fluid, *A* is the surface through which flow occurs and k is the permeability of the porous medium. In fractured media, in case of a single fracture, the permeability parallel to the fracture direction can be calculated using basic Poisseuille flow theory, assuming an aperture $\bar{w}$ between two parallel plates:

$$k_f = \frac{\bar{w}^2}{12} \quad (7)$$

This contribute to define the permeability tensor, which is assumed to be in a coordinate system with axes along and perpendicular to the fracture orientation, in order not to have off-diagonal elements.

The mechanical behavior of the whole rock-mass was governed by elasticity according to the linear and reversible Hooke's law. As Atkinson (1982) observed during his experiments, I assumed the subcritical propagation of cracks occurring when the stress intensity factor falls between an initial

value of stress intensity factor (K_{I0}), below which no crack growth is observable, and a critical value representing the fracture toughness (K_{Ic}), which is a measure of how long the crack will grow until the rock fails. To assess whether or not the model falls within the subcritical crack growth (SCG) window the stress intensity factor needs to be calculated. In an isotropic and elastic material, the stress intensity factor for a uniformed crack subjected to a far-field minimum stress σ_3 is:

$$K_I = P_{net}\sqrt{L\pi} \quad (8)$$

where P_{net} is the net pressure in the crack, corresponding to the difference between internal fluid crack pressure and minimum horizontal stress (P_f - σ_{min}), and L the half length of the crack. Within the SCG regime, the increase in crack length over time can be calculated using crack propagation velocity following Eq. (5). Consequently, the fracture average width $\overline{w}$ can be related to fracture length using a relation for cracks in an elastic material of infinite extent, subject to a constant internal pressure P_f, *and* an external confining stress σ_{min}, applied perpendicular to the crack plane (figure 7).

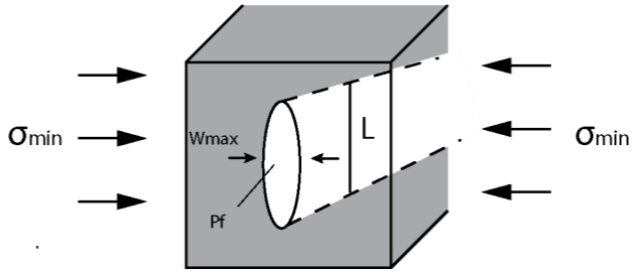

Figure 7: crack in a cubic zone. Picture from (Economides and Nolte 2000.

The formula for calculating the average width is the following:

$$\overline{w} = \frac{16P_{net}L(1-\nu^2)}{3\pi E} \quad (10)$$

Where *v* is the Poisson ratio, *E* the Young modulus.

5.2 Implementation of FLAC3D models

Fast Lagrangian Analysis of Continua in 3-Dimensions (FLAC3D) is a three-dimensional explicit finite-volume software for engineering mechanics calculations. This software, developed by Itasca Consulting Group, is particularly useful to simulate the mechanical behavior of soil, rock or other materials in three dimensions. Materials are modelled using polyhedral elements within a three-dimensional grid. Each element of the model behaves according to a user-defined linear or nonlinear stress/strain law and deforms as a consequence of the applied boundary conditions. The material can behave elastically, fail according to specified failure criteria, and flow according to specified creep laws. The finite element grid can deform according to the constitutive behavior of the represented material (Itasca Consulting Group, 2018).

With the built-in programming language FISH, I have implemented my constitutive model tailored at the coupled behavior and with the equations derived from Atkinson (1982) and Zurkhov (1984). Two models will be presented and analyzed in the following chapters: (1) a smaller model implemented with fracturing process and permeability changes, to simulate the subcritical crack growth evolution at laboratory scale, and (2) a field-scale model, without any fracture mechanics or permeability

changes, that is used to investigate conditions for initiation of subcritical crack growth around a geothermal doublet.
Numerical simulations were initialized by applying an external stress and internal fluid pressure boundary condition to the model in such a way that the model deformed elastically and reached the stress state equilibrium without yielding. Then fluid started to be injected into the system from a source nucleated within a particular zone in the model (figure 8). FLAC3D simulations involve a series of cycles, each of them including a series of flow steps were fluid was injected into the system and a new pore pressure field was generated, followed by mechanical steps, where a mechanical analysis was performed to retrieve poroelastic change in stress caused by the alteration of the pore pressure field. This step-wise calculation was performed to allow the model to maintain quasi-static equilibrium during the entire simulation.

5.2.1 Lab-scale model

The lab scale model was used to simulate the subcritical crack growth evolution at laboratory scale, and to assess the potential of such a process in enhancing the permeability of tight rocks.

The model represents a symmetric quarter of a cube of dimensions 0.075 x 0.075 x 0.15 m made up of 86975 zones all equal in dimensions. The high number of zones allows to have a better resolution and analyze with much details the processes happening at crack scale. The fluid injections were modeled over a single zone located in the middle of a corner edge as the response of the model to injection is expected to be symmetrical for isotropic reservoir properties.

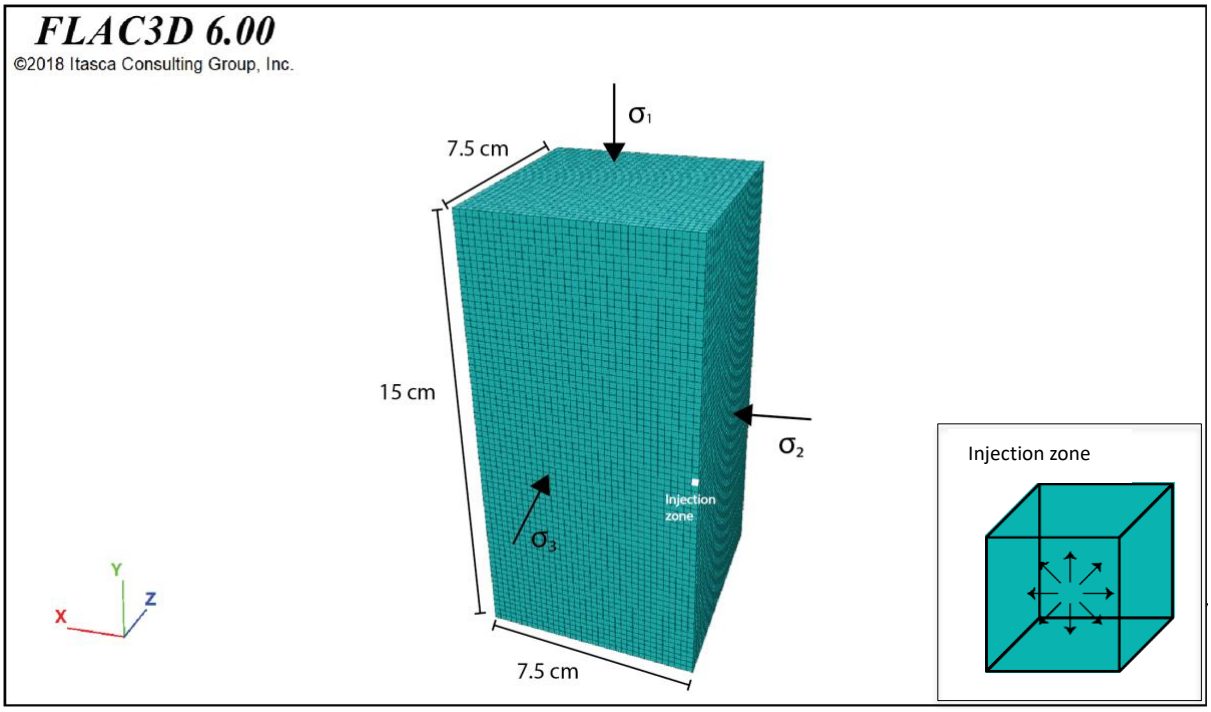

Figure 8: FLAC3D Lab-scale model geometry. The injection area in the model is highlighted by the white square and simply represented in the bottom left corner of the picture. In the injection area representation arrows represent the how to fluid flows away from the injection source.

A series of boundary conditions were applied during the simulation: stresses boundaries were applied along the y, x and z respectively, defining anisotropic stress conditions. A displacement boundary was applied to the bottom surface, not to allow it to move vertically during the whole simulation. Finally, the horizontal boundary surfaces have been set as impermeable, while the flow exchange between

the grid and the outside world was allowed across the top and bottom boundary surfaces. The simulation was carried out assuming the model to elastically behave, therefore only the elastic parameters were necessary for the mechanical analysis. The fluid flow was assigned as anisotropic, because the permeability anisotropy implies preferential flow directions in situ. A representation of the model is given in figure 8.

The mechanical analysis was performed to calculate the fracturing process and the relative permeability evolution within the model. A flow diagram used for simulations of the lab-scale model setup is shown in figure 9. To simplify the model and reduce computation time, a single crack was modeled and it was assumed that crack propagation started in the injection zone. In this zone an initial crack with length "L_0" was assumed to be present. Water was injected at a constant rate and, when the subcritical crack growth conditions were met, the crack started propagating and the permeability updated accordingly. To assess whether or not SCG conditions were met, the stress intensity factor K_I was cyclically computed by FLAC3D in response of P_{net} and crack length variation(c.f. equation 8).

Once the subcritical crack growth conditions were met in a particular zone, the crack growth velocity was locally calculated using the subcritical crack growth parameters experimentally determined by Ko (2008), and length of the crack was updated through the following equation:

$$L = L_0 + v * dt. \quad (10)$$

where L_0 is the initial value of crack length, v is the crack growth velocity (eq.6) and dt the time variation.

It is assumed that the crack grows following a preferred orientation perpendicular to the minimum principal stress. The orientation does not change during the simulation, i.e. potential rotation of principal stresses due to crack growth is neglected. The crack length value is then used for the computation of the fracture width $\overline{w}$ (Eq. 9) and used for the next calculation cycle. The permeability along the length of a crack for a zone with a crack extending over the full width of the zone was calculated before crack initiation using the arithmetic mean permeability of fracture and reservoir (matrix) permeability, weighted by the ratio between average fracture width and zone width:

$$k_{t1} = \left(\frac{\overline{w}}{zone_{width}}\right) k_f + \left(1 - \frac{\overline{w}}{zone_{width}}\right) k_0 \quad (11)$$

where $zone_{width}$ is the width of a single zone in the model and k_0 is the initial reservoir permeability. This equation is valid only for a zone with a crack extending over the full width of the zone (i.e. just before it crosses the zone boundary and starts propagating in the next zone). With this k_{t1} value, the permeability along the length of the crack (k_t) after each time step in a calculation cycle can be approximated if it is assumed that P_{net} remains constant:

$$k_t = k_{t0} + \frac{current\ crack\ length}{zone_{width}}(k_{t1} - k_{t0}) \quad (12)$$

Where k_{t1} is the value of permeability along the length of the crack retrieved from Eq. (11), and k_{t0} the value when the crack starts growing (at the beginning corresponding with the reservoir permeability value). The new permeability value is then used to update the permeability tensor in the directions parallel to the crack growth direction, while the permeability perpendicular to the crack growth direction is assumed to not change during the simulation.

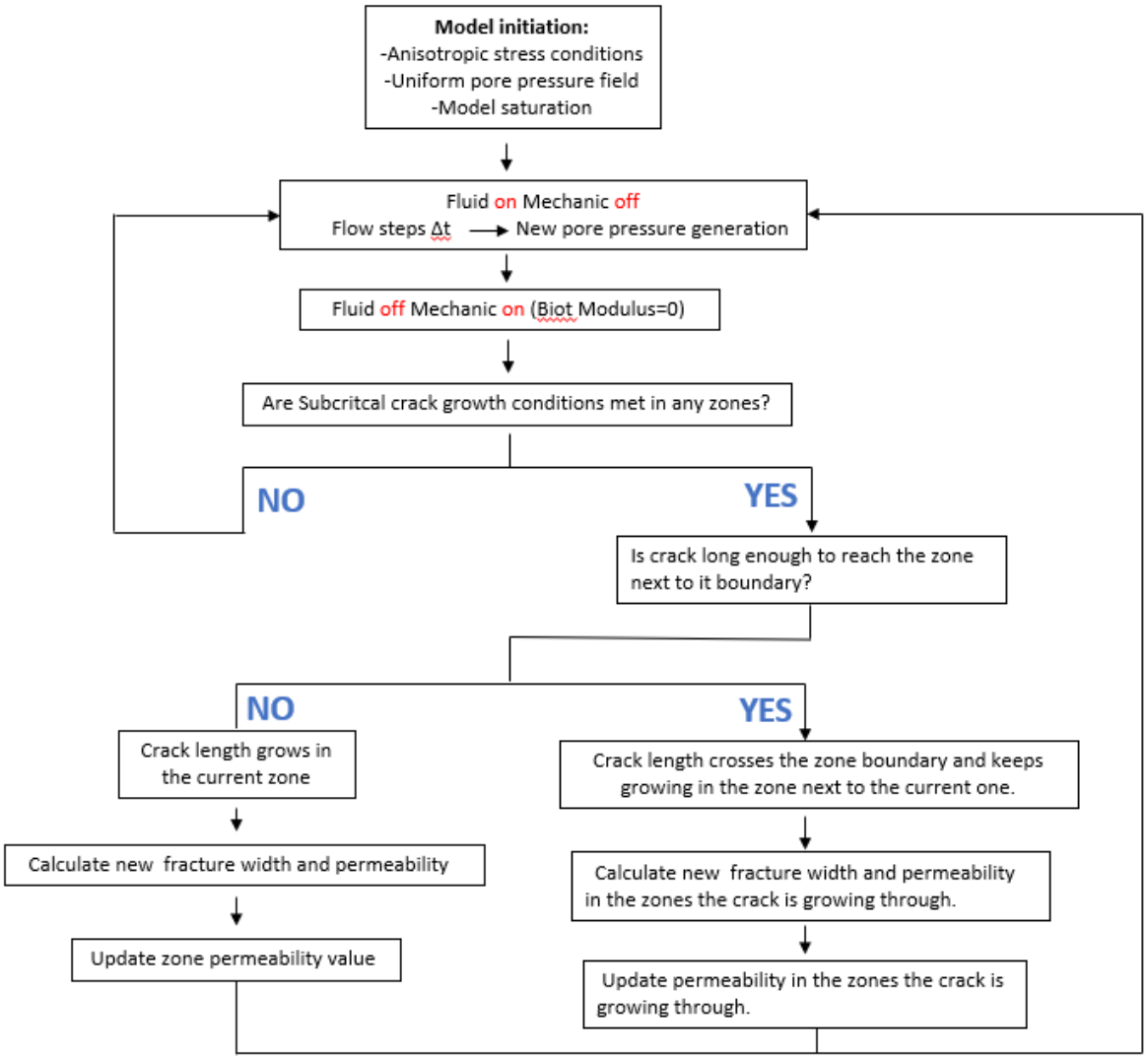

Figure 9: Lab-scale model flow chart of FLAC3D implementation. In the approach a zone is a single element in the finite element grid.

When the crack length reaches the zone width, it extends into the adjacent zone. Consequently, permeability along the length of the crack in the new zone will be updated following the procedure described above. As crack width continues to increase with propagation of the crack, the permeability along the crack in the first zone is also updated using Eq. (12). The equations used to calculate the crack geometry and the final zone permeability were implemented through a dedicated algorithm (using the FISH programming language incorporated in FLAC3D).

5.2.2 Field scale model

The field scale model was used to simulate the spatial and temporal distribution of pressure and stress during doublet fluid circulation involving an injection and production well. Only poroelastic stress changes were considered. The distribution of pressure and stress was used to determine areas where conditions are favorable for subcritical crack growth and initiation of cracks may be expected. Different simulations with different injection and production rates were modeled, to assess how the flow rate influences the initiation of cracks. The model simulates the early stages of typical doublet operations, particularly focusing on the horizontal fluid flow but neglecting thermal effects. The aim was to analyze the pressure conditions within the zones next to the injection area and assess the condition for SCG initiation of over time.

The model represents a 2000 x 1000 x 10 m layer at a depth of approximately 4 km, made up of 900 zones in total. The injection and production zones are located at a distance of 1000 m between each other. These zones are located at the boundary of the model to reduce the zones number by modelling only half symmetry and save calculation steps, but still having the opposite boundaries from the injection sources far enough not to influence the pressure field evolution. The zones number and size have been redefined close to the wells to have a higher resolution on the processes which occur near the injection areas. Injection rates were small in the initial cycles and gradually increase until the desired rate was achieved. After that water was injected in the model at a constant rate. This was done to maintain a quasi-steady equilibrium during the initial stages and limit the pressure changes between subsequent timesteps. Horizontal flow boundaries were permeable and vertical boundaries were set as impermeable so potential effects of flow in vertical direction is neglected (i.e. a permeable reservoir with impermeable top and bottom seals is modelled with negligible flow in vertical direction). A representation of the model is given in figure 10.

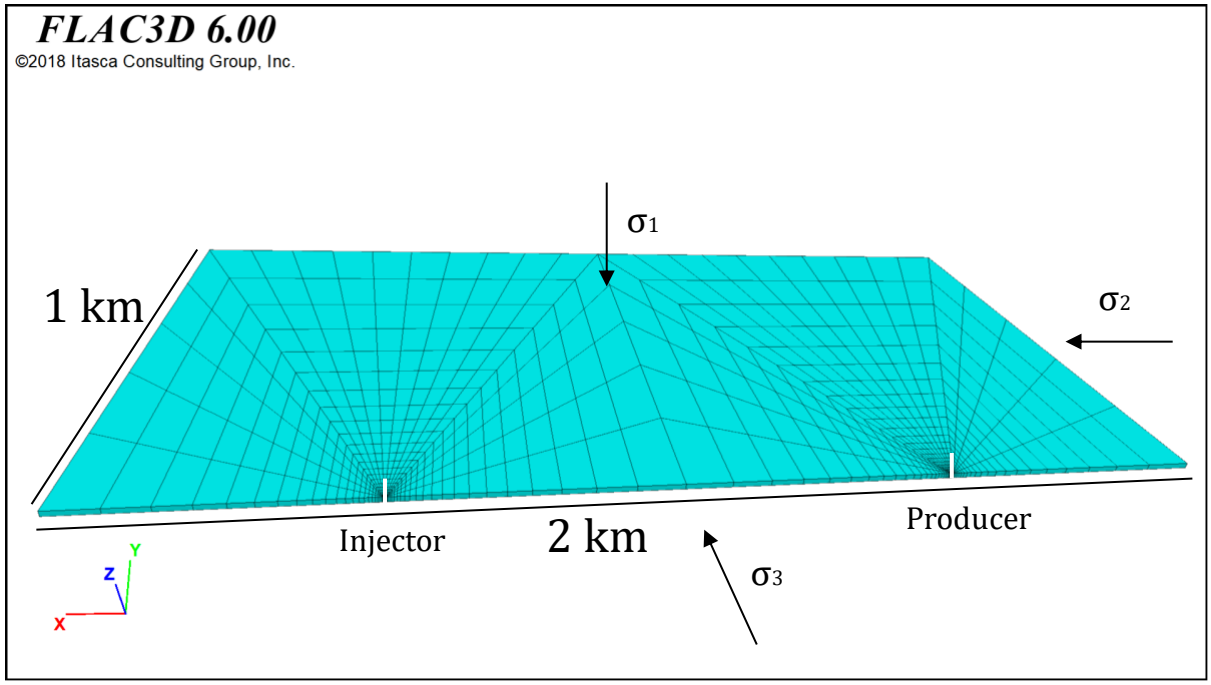

Figure 10: Geometry of the field-scale model.

Structural boundaries conditions were applied to the model boundaries. Initial displacement constrains and initial stress boundaries were set on all the surfaces, and stress initialization was performed (Table 3). Stress conditions were then applied along the y, z and x axis to mimic the respectively σ_1, σ_2 and σ_3 calculated at reservoir depth. An initial value of pressure in the pores was also set, consistent with the assumption that the model was fully saturated at the beginning of the simulation. The model was assumed to behave elastically throughout the entire simulation. Poroelastic effects are modelled by setting bulk and shear modulus (Table 3).

Permeability was assumed to be isotropic and constant in all the directions during the entire simulation. The field scale model does not explicitly simulate crack propagation but rather simulates pressure and stress evolution around the wells. Therefore, permeability was chosen to be isotropic and is only relevant to investigate the initiation of the SCG process. Analysis of initiation of SCG is based on pore pressure and stress derived from the FLAC3D model in combination with relations for stress intensity factor and Mohr circle analysis. The initial crack length (L_0) was assumed to be constant in relations for the stress intensity factor.

The flow diagram for simulations of the field scale model is shown in figure 11. The pore pressure distribution in the FLAC3D model was validated using the doublet flow simulator DoubletCalc2D (TNO 2014 R11396). Doubletcalc2D is developed by TNO to calculate the temperature and the pressure evolution during operation of geothermal systems consisting of two or more wells over the lifetime of geothermal projects. In the FLAC3D simulations constant temperature was assumed so that viscosity and density of the fluid are constant.

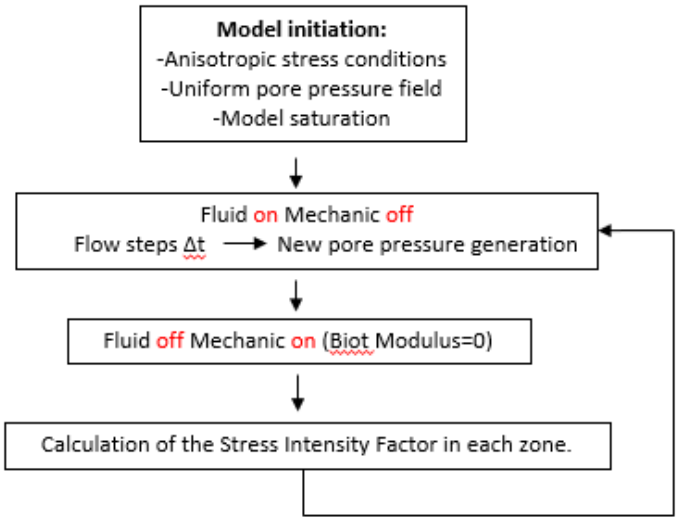

Figure 11: Field-scale model flow chart of FLAC3D implementation.

An overview of all the parameters used in the model is given in table 3. Fluid injection and production was modelled for a total period of 1 year. Four main scenarios have been simulated, each of them presenting a different injection and production rates. Injection and production rates were kept constant throughout each simulation.

5.2.3 Models input parameters

Initial values of permeability and porosity in the models were set as those measured by Felder (2018) during Trias Westland reservoir core measurements. Porosity value was established not to change during the numerical simulation and the Biot coefficient was also constantly kept 1 following the assumption that changes. in stress due to pressure changes are fully accommodated by the pore fluid. In order to obtain the best response from the model a sensitivity analysis was performed. This analysis

was particularly useful to determine the ratio between initial crack length value and the model zone length and the subcritical crack growth parameters. After few simulations, the best results have been achieved with the zone length being 0.001 m larger than the initial crack length "L_0". The SCG is a slow process and this ratio between zone length and initial crack length has resulted appropriate to analyze the crack growing through multiple zones and, as a result, to achieve permeability contours away from the injection area. The subcritical crack growth parameters determine the growth rate of the crack. These parameters were taken from previous experiments on Coconino Sandstone (see Ko 2008). From these experiments Ko (2008) retrieved an average value of 1.73 x 10^{-1} m/s for the pre-exponential SCG constant A (see equation 4). According to Ko (2008), subcritical exponent "n" values in Coconino Sandstone range between approximately 10 and 50. According to these values, three different scenarios for crack growth velocity have been proposed for three different values of the SGC exponent "n". The relations between stress intensity factor and crack propagation velocity for the three cases are presented in figure 12.

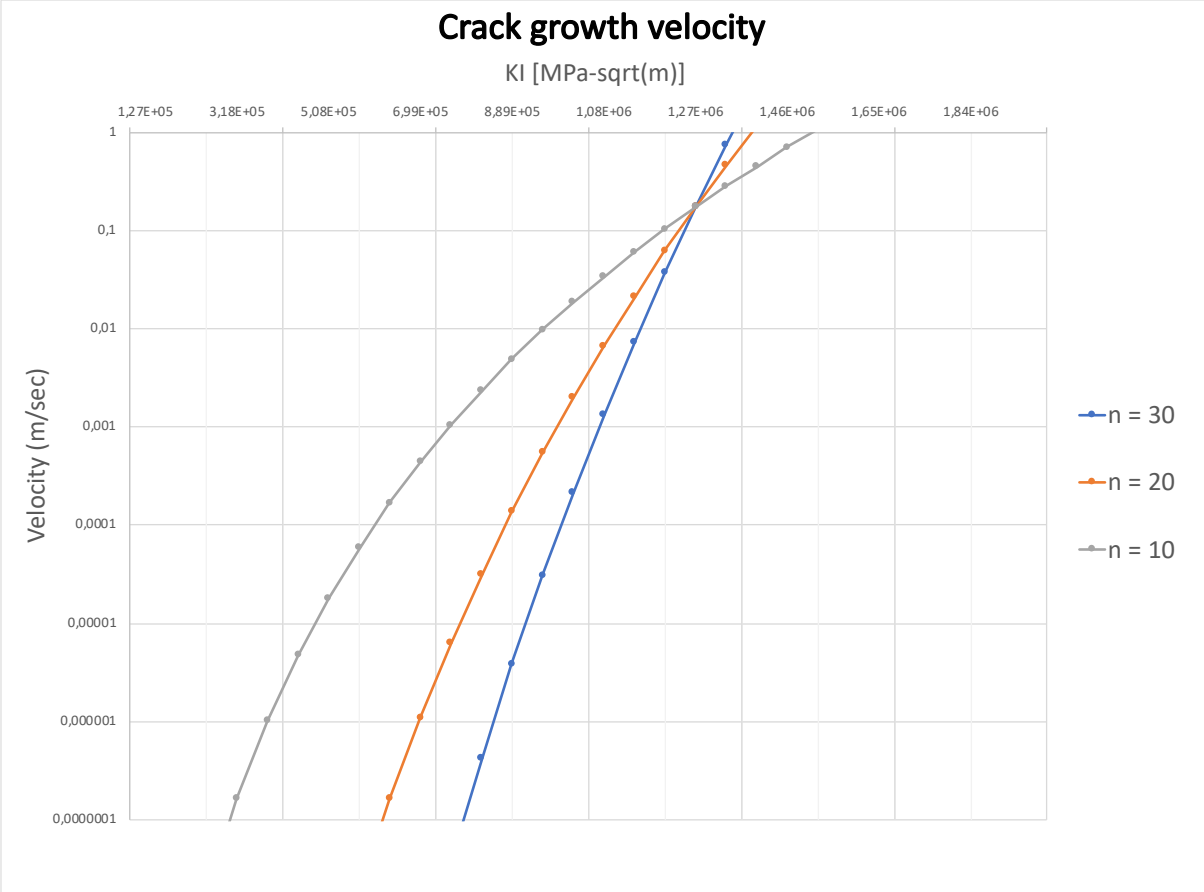

Figure 12: Crack velocity growth for three different value of the SCG index "n" data from Ko (2008).

After a sensitivity analysis, a value of 10 for the SCG index has been chosen among the values proposed by Ko (2008) for different samples . This value has been considered to be more appropriate, because it allowed the crack to considerably grow even at lower values of K_I and consequently saves time during the model calculation. Flow time steps of 1 s each were adopted to model the SCG. This to minimize numerical instabilities between each step and to have a better resolution on the crack evolution overtime. An average value of 1.27 MPa*$m^{1/2}$ for fracture toughness (K_{IC}) of sandstone has

been assumed (Senseny et al. 1984), and the initial stress intensity factor (K_{I0}) was calculated accordingly. An overview of the parameters used in the model is shown in table 3.

Lab-scale and Field-scale model parameters		
Parameter	**Lab-scale simulation**	**Field-scale simulation**
G (shear modulus)	*5.08 GPa*	*5.08 GPa*
K (bulk modulus)	*4.9 GPa*	*4.9 GPa*
Porosity (ϕ)	*4%*	*4%*
Initial Permeability (k0)	*0.1 mDa*	*0.1 mDa*
Fluid Modulus	*2×10^{9}*	*2×10^{9}*
Initial Crack Length	*0.001 m*	*0.001 m*
Fracture Toughness	*1.27 MPa*m $^{1/2}$*	*1.27 MPa*m $^{1/2}$*
σ_1	*90 MPa*	*90 MPa*
σ_2	*64 MPa*	*64 MPa*
σ_3	*60 MPa*	*60 MPa*
Pore Pressure	*40 MPa*	*40 MPa*

Table 3: Parameters used during the FLAC3D numerical calculations.

6. Results

6.1 Results of the lab-scale model in FLAC3D

6.1.1 Stress intensity factor evolution and permeability changes

For a constant injection rate of 1.8×10^{-5} l/s the stress intensity factor "K_I" evolution, calculated in the same zone where the fluid is injected, is shown in figure 13. After approximately 28 hours of simulation, because K_I in the injection zone has already reached a value of 1.93×10^5 Pa*m$^{1/2}$, the crack has already entered in the SCG regime and started propagating. Although the permeability tensor is already being updated for the zones the crack is growing through, 28 hours are not sufficient for the SCG to enhance permeability significantly. After 45 hours of simulation, K_I has reached a value of 2.5×10^5 Pa*m$^{1/2}$, meaning that the conditions for subcritical crack propagation are still satisfied.

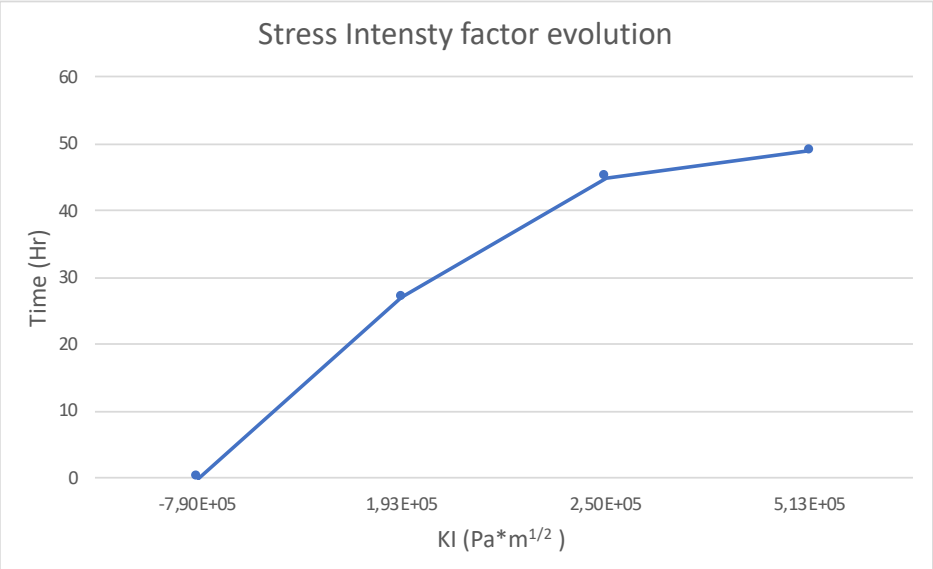

Figure 13: Evolution in time of intensity factor (KI) in the injection zone.

The average fracture width, automatically calculated, is now sufficiently large to produce relevant permeability change in the involved zones, as can be seen in figure 14a. Permeability contours show a maximum increase up to 0.7 mD around the injection source.

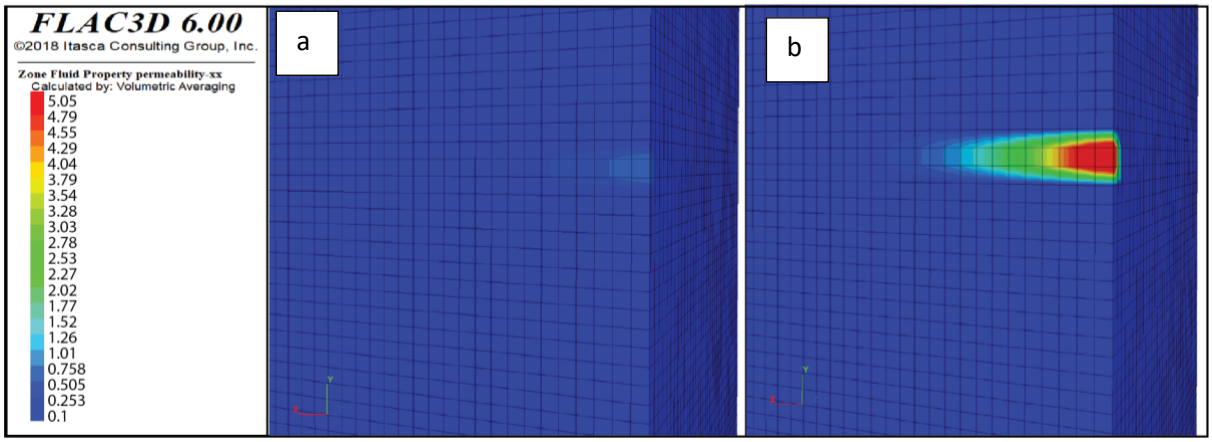

Figure 14: Evolution of permeability (mD) parallel to the x direction over time.

From now on outputs have been calculated more often to have a better resolution on the crack growth and relatively permeability enhancement. Around 49 hours after the beginning of the simulation, the stress intensity factor has reached a value of 5.13 x 10^5 Pa*$m^{1/2}$ (figure 13). The remarkable crack length increase creates permeability contours which extend further away from the injection source, meaning that the crack has growth through several zones. The values of permeability displayed after 49 hours from the start of the injections suggest a maximum value of permeability around the injection source of 5.05 mD (figure 14b), representing a local increase of approximately 5000% from the value of reservoir permeability(0.1 mD). Furthermore, even at approximately 2 cm away from the injection point, the zones present permeability values of around 1.0 mD, meaning that the crack has already significantly grown through those zones.

6.1.2 interpretation of the lab-scale model results

The results obtained by the lab-scale model give an overview on the effects of time-dependent subcritical fracture propagation on permeability. The aim has been to explore methods to implement the fracturing process and permeability changes in numerical finite element models (FLAC3D). Many assumptions were made that are still subject to discussion (i.e. mainly proper implementation of the fracturing process that is fully coupled with respect to mechanics and flow). A simplified method to link the evolution of cracks at small scale to permeability has been explored. Given the very low reservoir permeability of the modelled reservoir (0.1 mD), SCG conditions are already met within the injection zone after 28 hours of injection at very low injection rates . After SCG conditions are met, the crack starts propagating at subcritical velocities and permeability along the length of the crack increases. To visualize the Pore Pressure and the relative poroelastic effect on the total minimum (σ_3) and maximum (σ_1) principal stresses, effective stresses σ_3' and σ_1' around the injection source are retrieved from FLAC3D computations and plotted in a Mohr-Coulomb diagram and compared to a Mohr-Coulomb-Griffith failure criteria. Values of Cohesion and angle of internal friction are 16.5 MPa and 25°respectively (Ko 2008). In this study mode I crack propagation is analyzed (tensile mode only),

and shear failure is not be taken into account . The initial tensile strength value (T_0) can be related with the fracture toughness (K_{IC}) using the following relation proposed by Economides et al., 2010:

$$T_0 = \frac{K_{IC}}{\sqrt{\pi * a_c}} \qquad (13)$$

where a_c is a length scale (e.g. flaws) which in this case corresponds to the initial crack length value "l_0". Resolving equation n.13 the initial value of tensile strength results to be approximately 20 MPa.

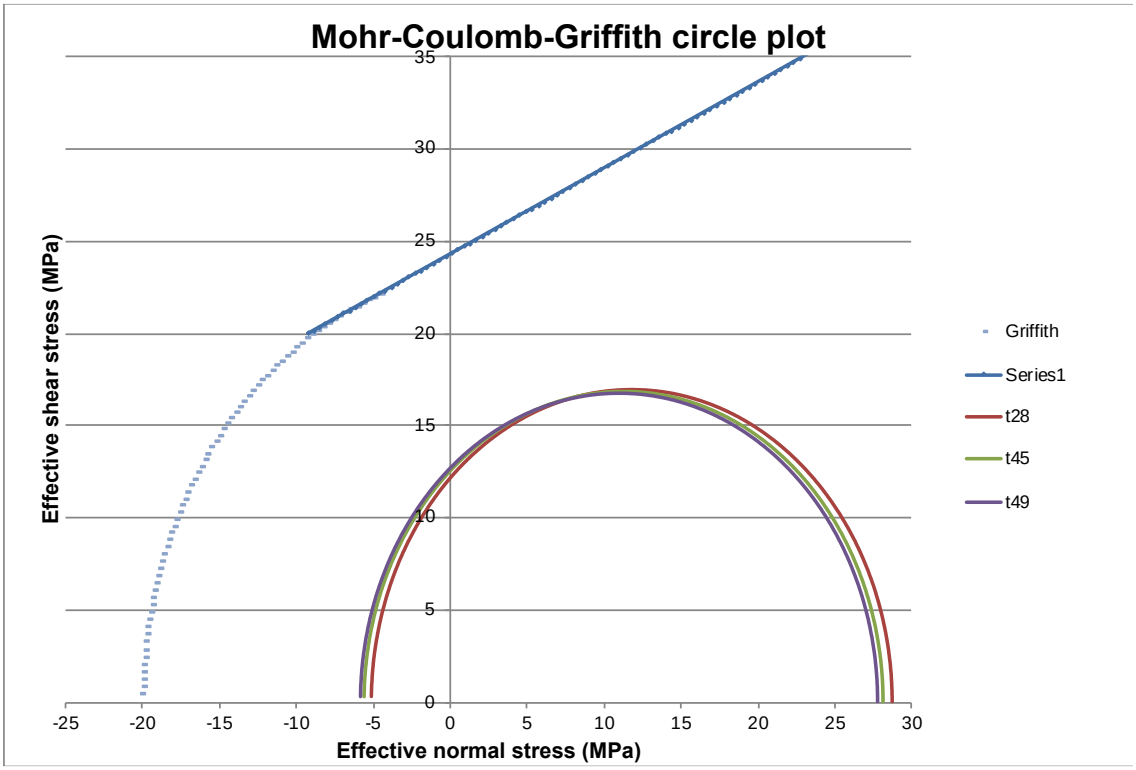

Figure 15: Mohr-Coulomb-Griffith envelope representing the evolution of effective stresses within the injection zone.

The state of stress relative to the injection zone is shown in figure 15. As fluid is kept injected in the model, pore pressure rises, and the effective stresses decrease. Minor changes in stress state are observed, because after 28 hours pore pressure had already almost reached steady state and effective stresses were not significantly affected anymore. The poroelastic response of the porous rock can be observed by shrinking of the Mohr circle with time. All the plotted circles fall within the subcritical crack growth regime(figure15), which confirms the observation made during the result analysis. In fact, all the values of σ_3' are lower than -3 MPa (larger tensile stresses), which represents the lowest σ_3' value to enter the SCG regime retrieved by calculating the "P_{net}" for the critical value of stress intensity factor "K_{I0}" (c.f. equation 8). Furthermore, no initiation of shear fractures occurs under these conditions as is illustrated by the fact that all the circles are plotted below the failure curve.

Because pore pressure tends to be constant as steady-state flow is approached for the current implementation of SCG, crack aperture and relative permeability are only dependent on crack length. This can be observed by comparing figure 13 and figure 15. Although changes in values of pore pressure and total minimum (σ_3) are not relevant, stress intensity factor "K_I" is still significantly increasing by an amount proportional to crack length (c.f. equation 8). Crack length keeps growing cyclically at a rate which increases with crack length (c.f. equation 5 and 8).

Under the conditions analyzed, the crack length is equal 1.8 x 10^{-3}m, growing with an approximate velocity of 1.2 x 10^{-9} m/s ~28 hours after from the beginning of the simulation. After ~45 hours, the crack length has reached 2.21 x 10^{-3} m, and the effect on permeability starts to be perceivable (figure 14a). The rate at which the crack is growing is then 1.5 x 10^{-8} m/s, more than 1 order of magnitude faster compared to crack propagation velocity at 28 hours. After 49 hours the crack length has reached a value of almost 1 x 10^{-2} m. At this point permeability in the zone adjacent to the near well zone (>2 x 10^{-3} m distance from the well) is affected (figure 14b). The crack velocity has reached ~2 x 10^{-5} m/s.

Subcritical crack growth occurs under the conditions investigated during the numerical simulation, but the effect on stress state and permeability is limited. However, implementation of other conditions in the future may yield higher or more complex fracture patterns and larger effects on permeability might occur.

6.2 Results of the field-scale model

The variation in injection rate between different scenarios helps assessing injection pressures that lead to conditions that favor subcritical crack growth near the wellbore for a given set of reservoir properties (Table 3). The four scenarios describe four main situations. Scenario 1 describes a situation where the values of pressure within the reservoir are not high enough to reach the SCG conditions, deformation is fully elastic, and flow is at steady state. Scenarios 2 and 3 describe situations where SCG conditions are met within some zones close to the injection well. Scenario 4 describe the situation where a high injection rate causes pressure in the reservoir exceed the fracturing pressure and reach conditions for conventional fracturing. Results of the simulations for the four scenarios are described below.

6.2.1 Case 1

For an effective constant injection rate of 1 x 10^{-2} l/s, modeled over 1 year, the development of pressure field around the two wells is shown in figure 16. Figure 16a shows the PP field calculated by the partially coupled analysis in FLAC3D, while 15b one represents the outputs of the DoubletCalc calculation used to benchmark the FLAC3D results. After 1 year of continuous injections, the pore pressure around the injection area in the FLAC3D model has increased by 20.6 MPa, in respect to the initial reservoir pressure of 40 MPa. Similarly, The DoubletCalc model shows a total increase of 200 bar (≈20 MPa) around the injection well. The same amount of pore pressure change can be observed around the production wells in both models. However, because fluid is extracted, pore pressure decreases. The two models show very close results, even if they present slightly different geometry and DoubletCalc does not take into account any mechanical analysis, while FLAC3D does.

To establish the favorable conditions for SCG initiation in the model, the Stress Intensity Factor "K_I" has been continuously calculated for each zone. Because the conditions for SCG are expected to be reached where pore pressure is highest, the outputs for the K_I calculations have been recorded and analyzed only for the zones around the injection source. An overview of the main results in time is shown in figure 17.

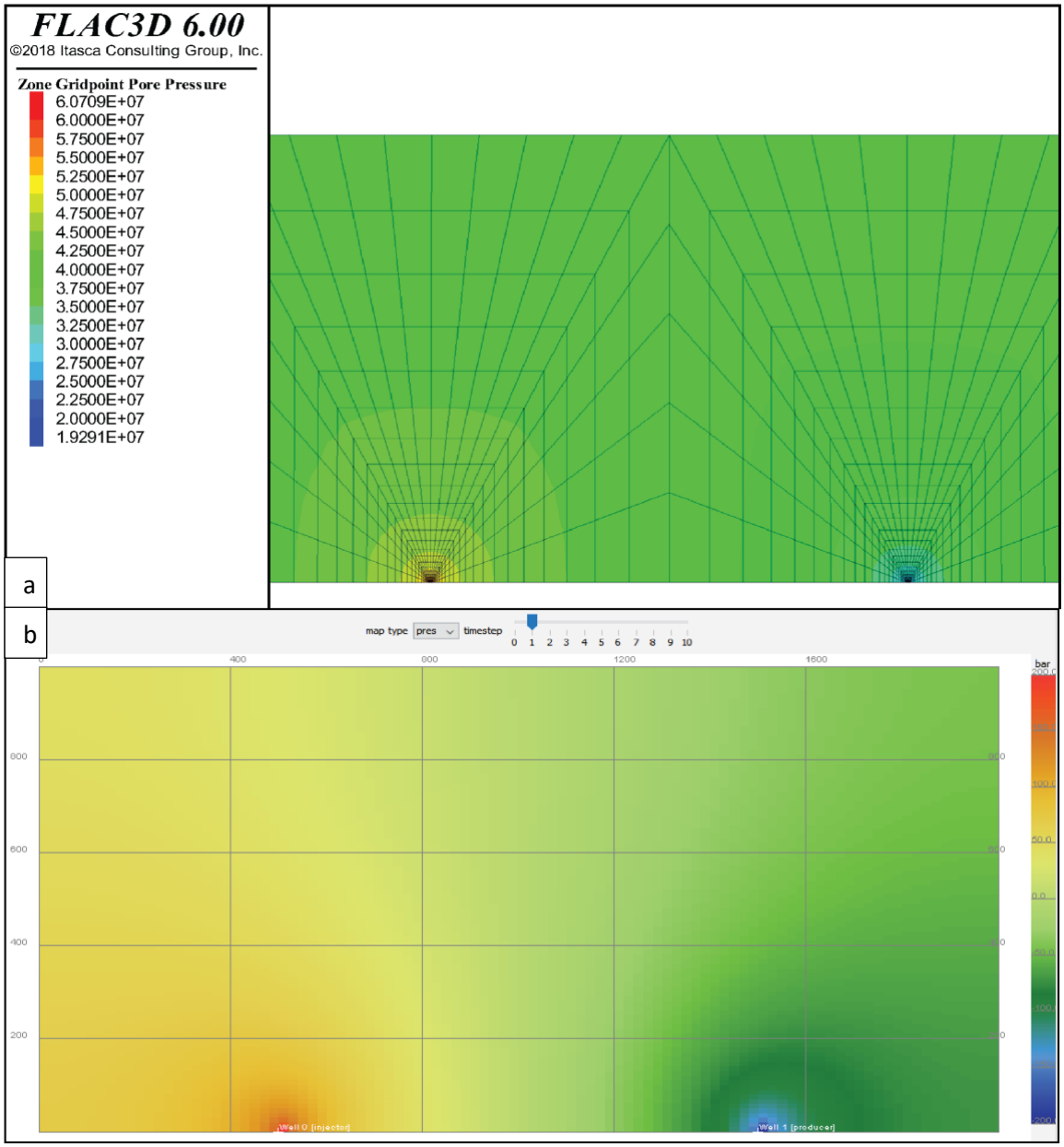

Figure 16: a) pore pressure field after 1 year calculated by FLAC3D; b) pore pressure field after 1 year calculated by DoubletCalc. These simulations have been carried out with a constant flow rate of 1 x 10^{-2} l/s.

Since the initial length is assumed to be constant until K_I becomes larger than K_{I0}, the stress intensity factor increase at the beginning is only dependent on the pore pressure (PP) and the minimum horizontal stress (σ_3). These two values are calculated in each timestep or calculation cycle by the model and used together with Eq. (8) to calculate the stress intensity field in each zone. Is it observed that the increase in K_I occurs mostly in the zones next to the injection source, where changes in PP and σ_3 are largest. However, at this injection rate, pore pressure near the injection area never exceeds (σ_3). For this reason, K_I never becomes larger than threshold "K_{I0}" of 1.27 x 10^5 Pa*$m^{1/2}$, therefore no subcritical crack growth occurs within any zones in this case study.

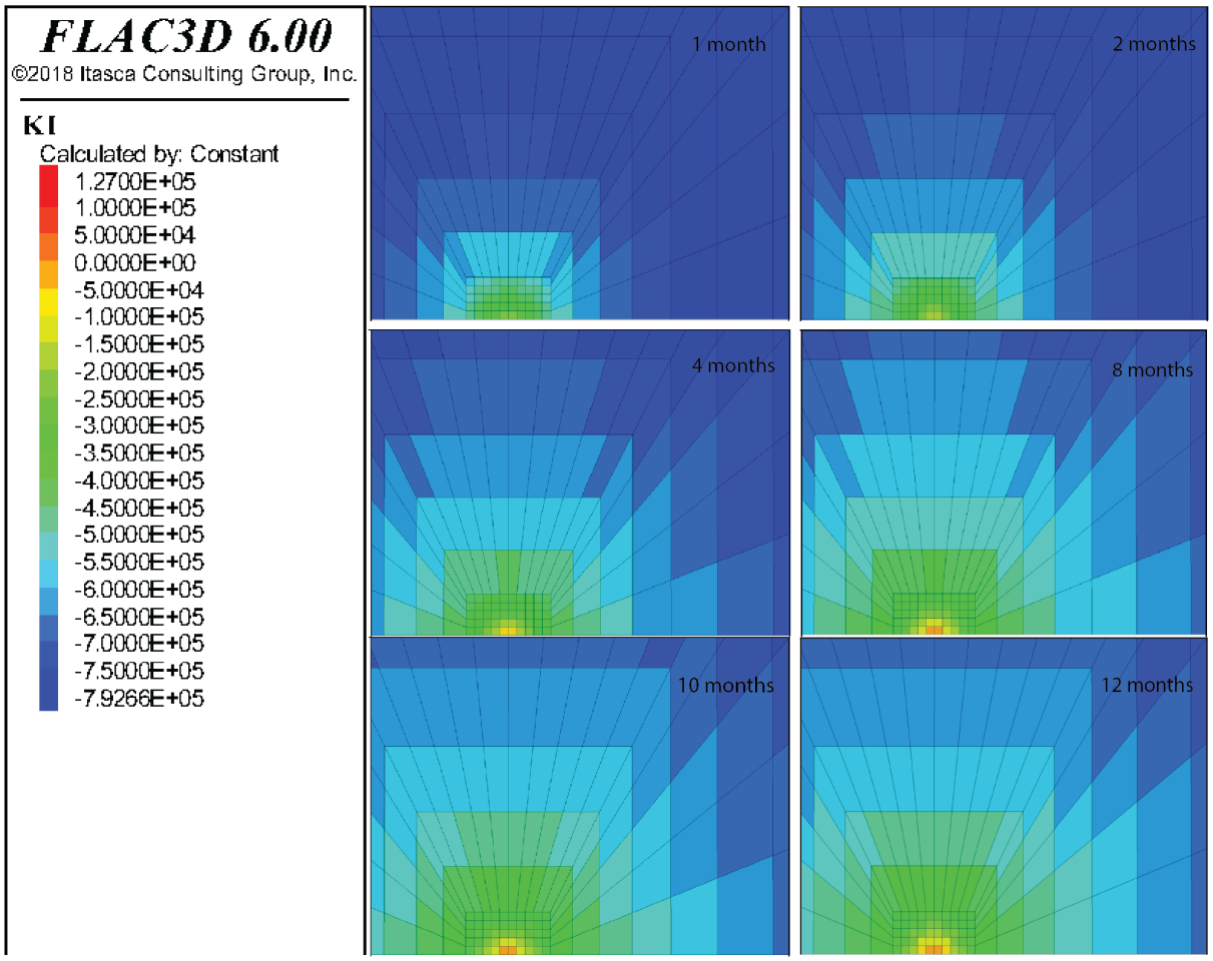

Figure 17: Stress intensity factor evolution calculated by FLAC3D for case 1.

6.2.2 Case 2

Since the previous simulation has shown no SCG behavior in the model, the injection rate in the second case/scenario has been increased to 1.2 x 10^{-2} l/s. Injection is again modeled at constant injection rate for 1 year and pore pressures are checked against DoubleCalc simulations again. After 1 year, FLAC3D shows a maximum reached pore pressure value of approximately 65 MPa around the injection area and a value of 15 MPa near the producing area, both representing a local change of 25 MPa. DoubletCalc shows a maximum pore pressure value of 250 bar (≈25 MPa) around the injection well and a respective decrease of minus 250 bar nearby the production well (figure 18). Again, results of the pore pressure field development are similar.

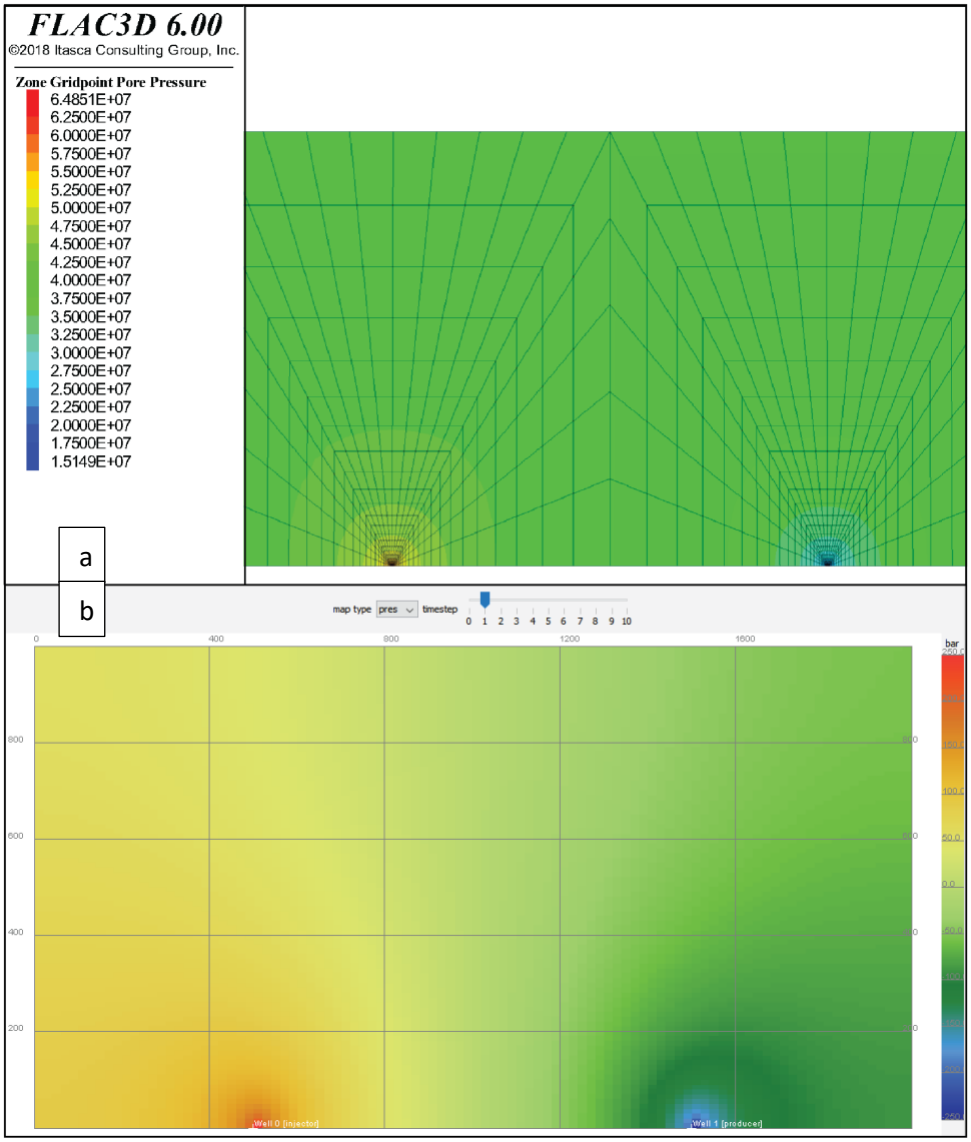

Figure 18: a) pore pressure field after 1 year calculated by FLAC3D; b) pore pressure field after 1 year calculated by DoubletCalc. These simulations have been carried out with a constant flow rate of 1.2 x 10^{-2} l/s.

As in the previous case, K_I has been monitored in each zone around the injection source. During this simulation, the injection rates were higher than in case 1 and PP was expected to reach higher values during the initial stages. For this reason, outputs have been printed out also for times corresponding to 10 days and 20 days after the beginning of the injections. The results show that SCG conditions are not met during the initial stages, although approximately after 2 months of constant injections, pore pressure values around the injection area are higher than σ_3. This is confirmed by a positive K_I, which reaches a value of 1.6345 x 10^4 Pa*$m^{1/2}$ within a radius of around 0.2 m away from the injection source. While fluid is kept being injected into the reservoir, at approximately 8 months from the beginning of the injections, the SCG conditions are reached within a radius of approximately 0.3 meters from the injection zones.

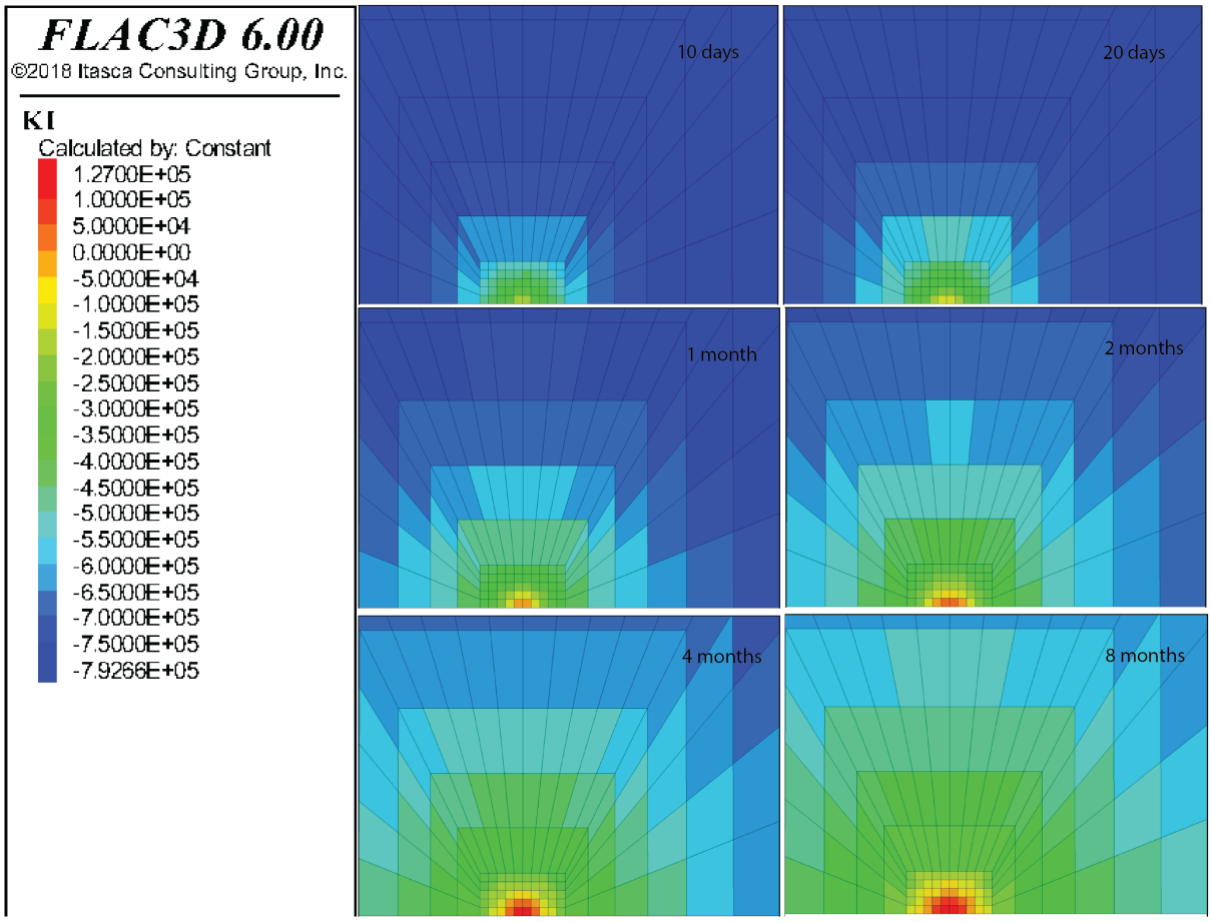

Figure 19: Stress intensity factor evolution calculated by FLAC3D for case 2.

6.2.3 Case 3

For the third simulation the used injection rate corresponds to a total value 1.4 x 10^{-2} l/s. After 1 year of constant injections the PP value around the injection source in FLAC3D has increased of approximately 29 MPa (figure 20a). DoubletCalc shows a slightly higher value of 300 bars around the injection well (figure 20b). This difference of approximately 1 MPa is probably linked the different analysis performed by the two software. Again, DoubletCalc only accounts for flow, without taking into account any mechanics. While, in the partially coupled analysis performed by FLAC3D, the volumetric strain developed as a result of the mechanic analysis might slightly affect the pore-pressure field development.

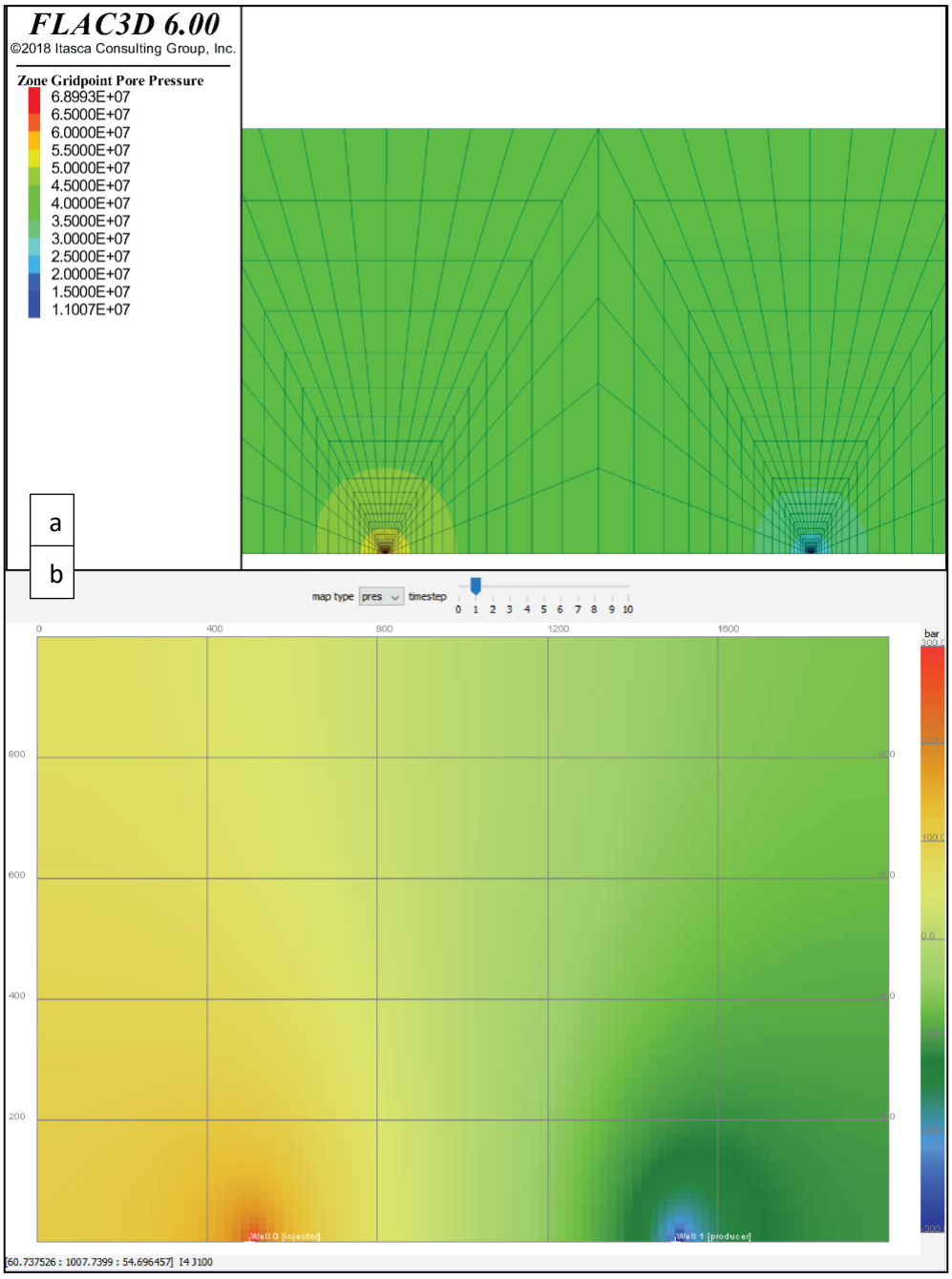

Figure 20: a) pore pressure field after 1 year calculated by FLAC3D; b) pore pressure field after 1 year calculated by DoubletCalc. These simulations have been carried out with a constant flow rate of 1.4 x

The K_I evolution during the FLAC3D simulation is shown in figure 21. The model has been again monitored more frequently during the first stages of the simulation. After a modeled time of 20 days, PP in the zones nearby the injection source is higher than σ_3, as can be observed by the positive value of K_I (3 x 10^4 Pa*$m^{1/2}$). As the simulation continues, K_I keeps growing in the model's zones reaching exceeding K_{I0} around 1 month from the starting of the injections.

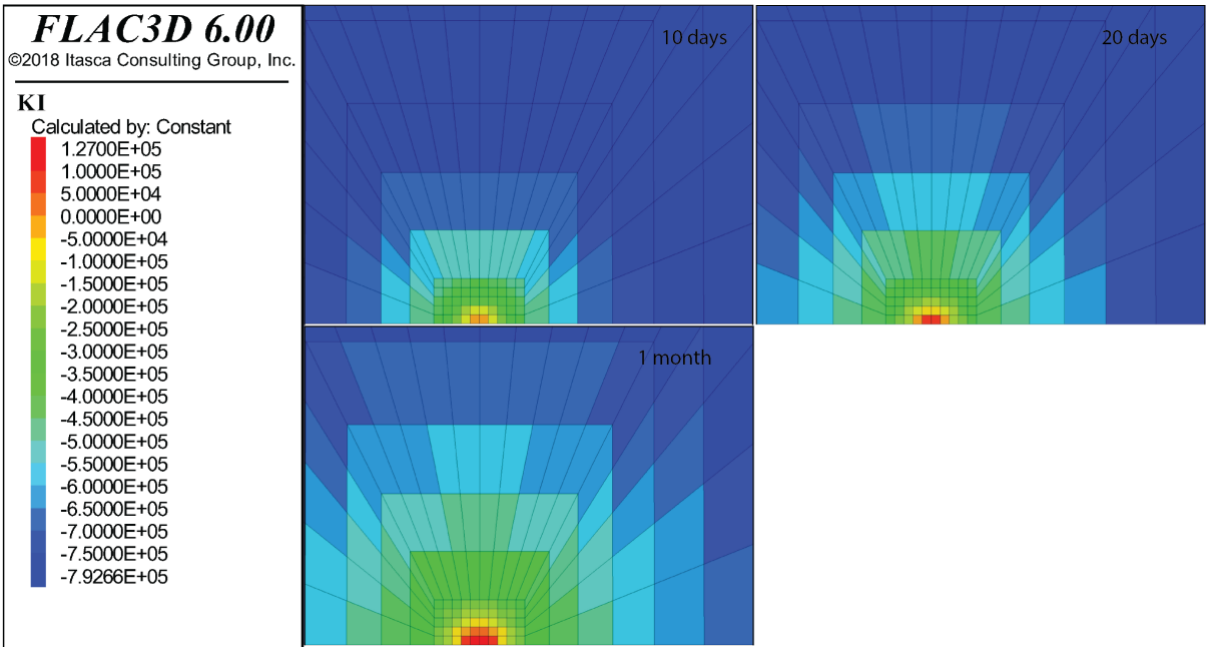

Figure 21: Stress intensity factor evolution calculated by FLAC3D for case 3.

6.2.4 Case 4

The last simulation was performed at a constant injection rate of 4 x 10^{-2} l/s. A relatively high rate was used in this case to test the model response especially during the initial stages where high PP values are expected to be achieved close to the injection area. Again, the DoubletCalc computation used to benchmark the FLAC3D model gives acceptable results. The misfit between the maximum PP values nearby the injection area in the 2 models is only 2 MPa (figure 22 a & b). A higher difference in comparison to the previous scenario was expected because of the higher volumetric deformation present in case 4 rather than case 3.

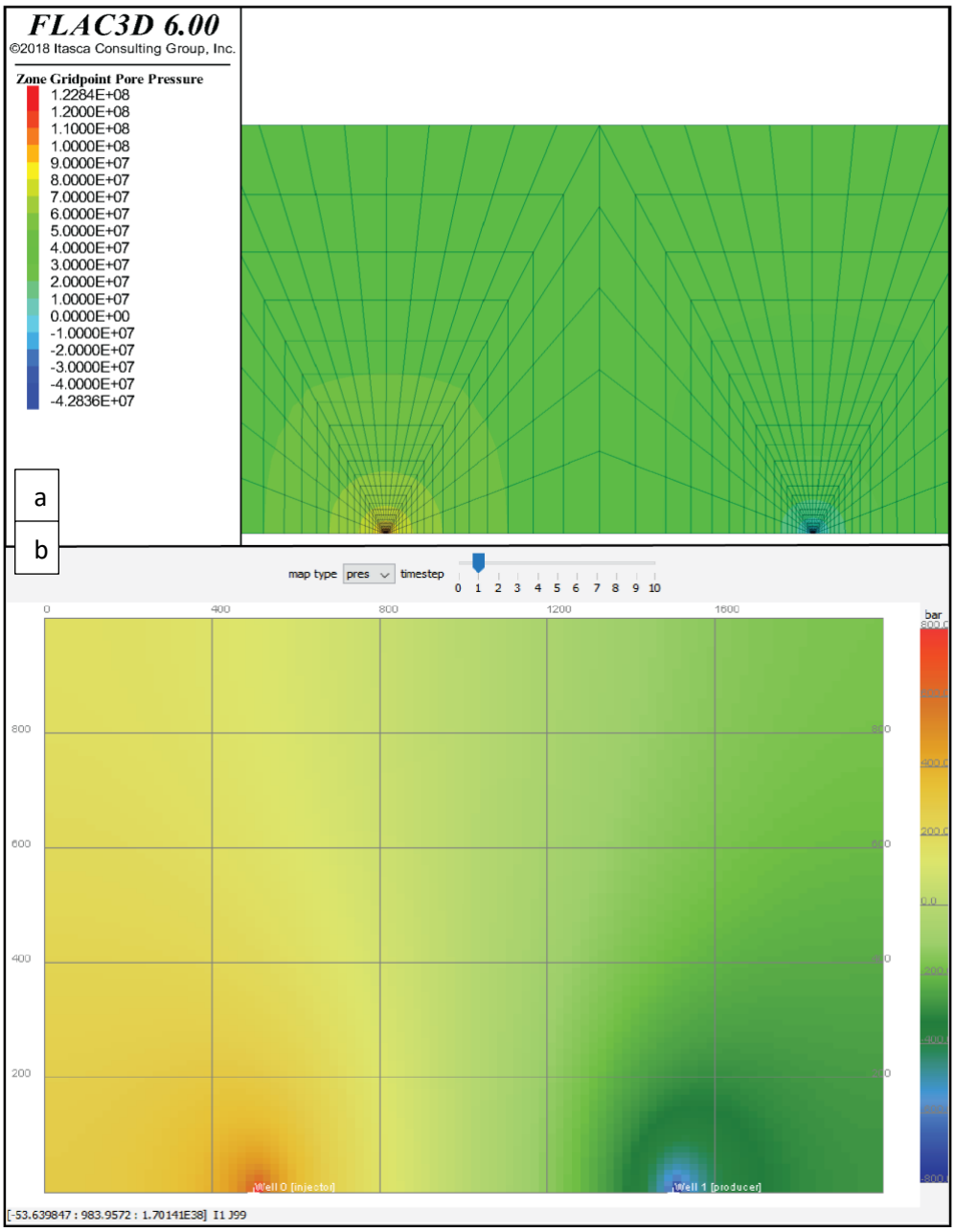

Figure 22: a) pore pressure field after 1 year calculated by FLAC3D; b) pore pressure field after 1 year calculated by DoubletCalc. These simulations have been carried out with a constant flow rate

By analyzing the values of figure 23, it is clear that higher injection rates reflect on a significant increase on the K_I values during the first stages in comparison with the previous modeled scenarios. After 10 days of constant injection rates, K_I in the zones close the injection source is already larger than Fracture toughness value (K_{Ic}), therefore the zones states are not within the SCG regime anymore, but within the conventional fracture criteria.

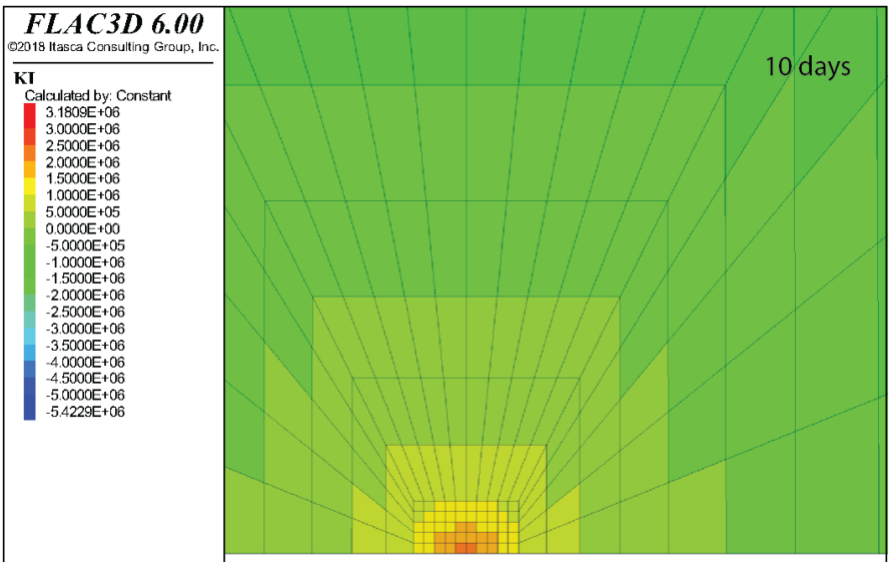

Figure 23: Stress intensity factor evolution calculated by FLAC3D for case 4.

6.2.5 Interpretation of the field-scale model results

The field-scale model results give a qualitative overview about the temporal and spatial distribution of pressure and stress changes which can be linked to criteria for initiation of (subcritical) crack propagation. Four different scenarios present different injection rates and associated pore pressure evolution. Although injection rates are still relatively low compared to conventional hydraulic fracturing treatments , pore pressure within the model ranges from 20 MPa for an injection rate equal to 1x 10^{-2} l/s in the first case, to almost 80 MPa for 4x10^{-2} l/s injection rate reached in the fourth case. The large pressure changes for small changes in injection rate are a consequence of low permeability (0.1 mD) of the reservoir.

The evolution of pore pressure relative to the far field stress promotes propagation of cracks . To analyze the stress state over time, and identify conditions for initiation of SCG, the effective stresses retrieved for each case from the FLAC3D computations have been plotted in Mohr Coulomb diagrams.

As can be seen in figure 24 relative to case 1, pore pressure increase over time makes the half circle shifting towards the tensile area of the graph. However, due to the small PP change during the simulation chosen elastic parameters, poroelastic effects are not really significant and differential stress (σ_1 - σ_3) is approximately constant . Furthermore, the relatively proximity of the vertical stress boundaries to the injection source, might affect the σ_1' calculation. After 12 months of continuous injections (t12), σ_3' has almost reached a negative value. However, since all the half circles are plotted below the failure curve no shear or tensile failure occurred within the year simulation.

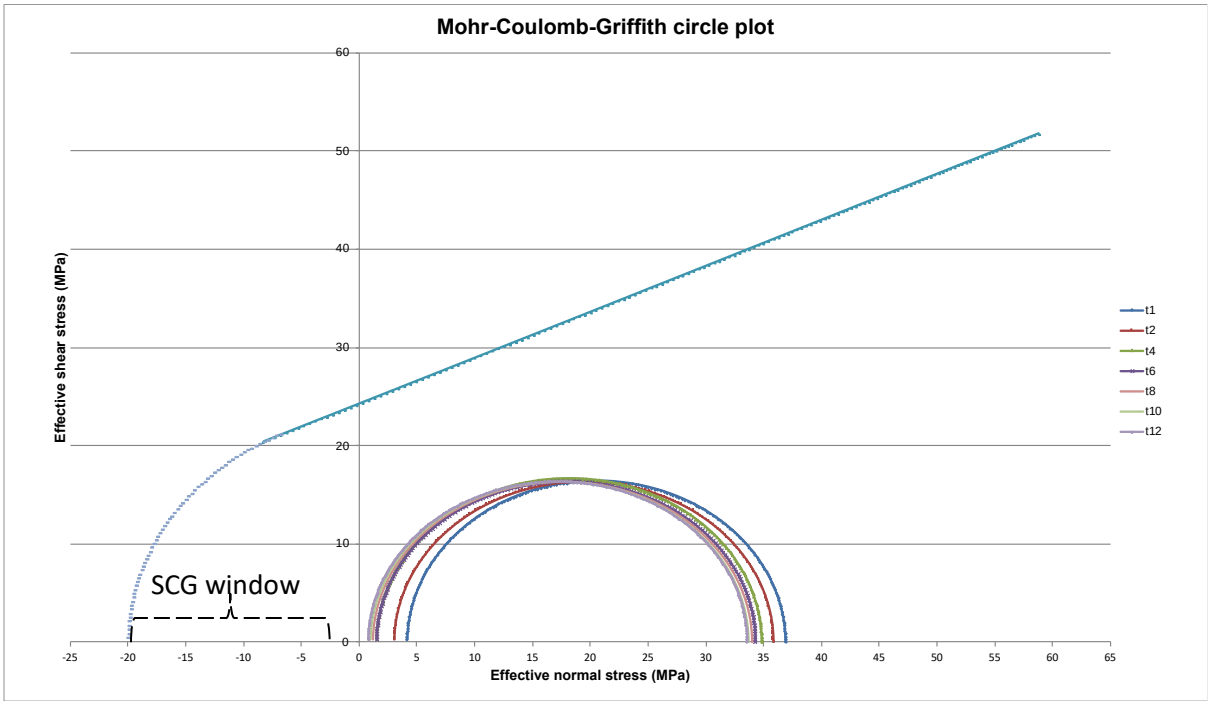

Figure 24: Mohr-Coulomb-Griffith envelope representing the evolution of effective stresses within a zone close to the injection source for case 1.

The second scenario presents a higher value of injection rates, therefore the half-circles are expected to be shifted more towards the tensile part of the plot (figure 25). As inferred by the FLAC3D computations for K_I, PP has overtaken σ_3 after 4 months of simulation, in fact σ_3' becomes negative and the correspondent half circle (t4) is partly inside the tensile regime of deformation.

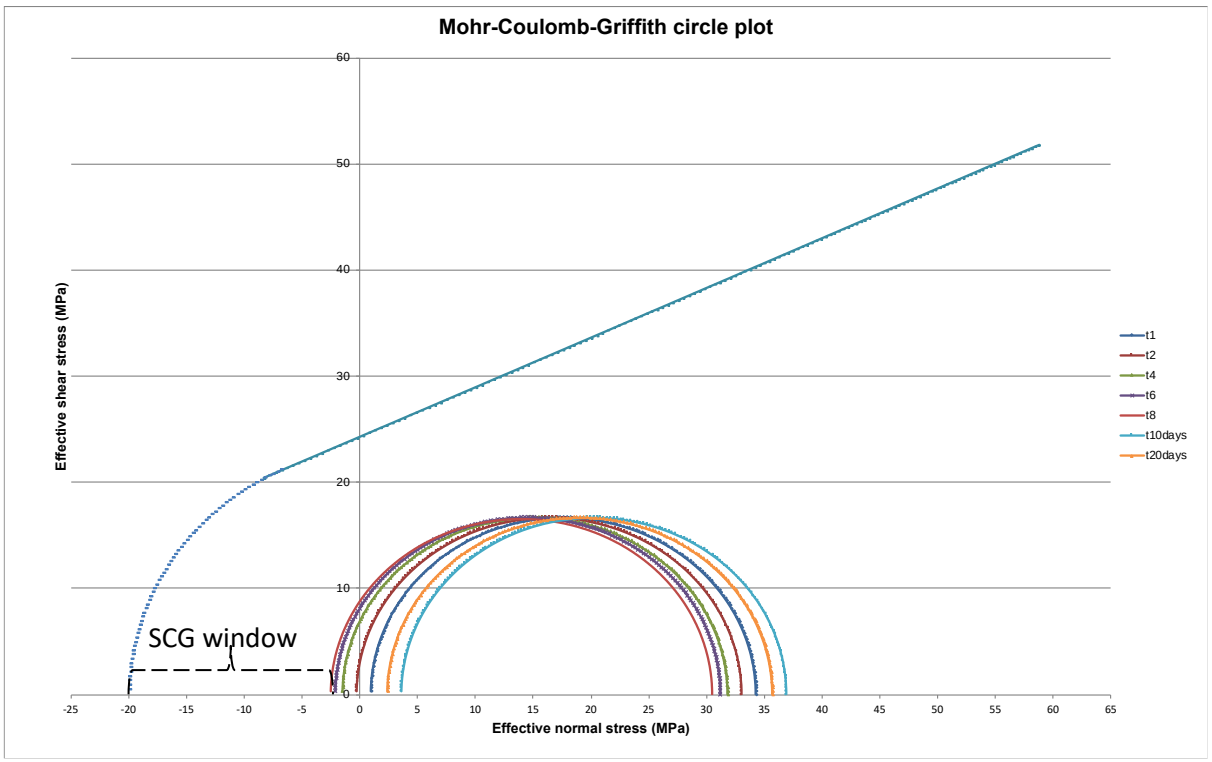

Figure 25:Mohr-Coulomb-Griffith envelope representing the evolution of effective stresses within a zone close to the injection source for case 2.

SCG conditions are achieved after approximately 8 months of continuous fluid injection, when K_I reaches a value of 1.4330 x 10^5 Pa*$m^{1/2}$. Within these conditions pre-existing cracks start propagating in a subcritical manner, because the half-circle (t8) is still below the failure envelope. Using equation 5, the velocity at which the crack will start growing can be estimated. Assuming SCG parameters as presented in figure 12 (n=10), the estimated velocity corresponds to 5.78 x 10^{-11} m/s.

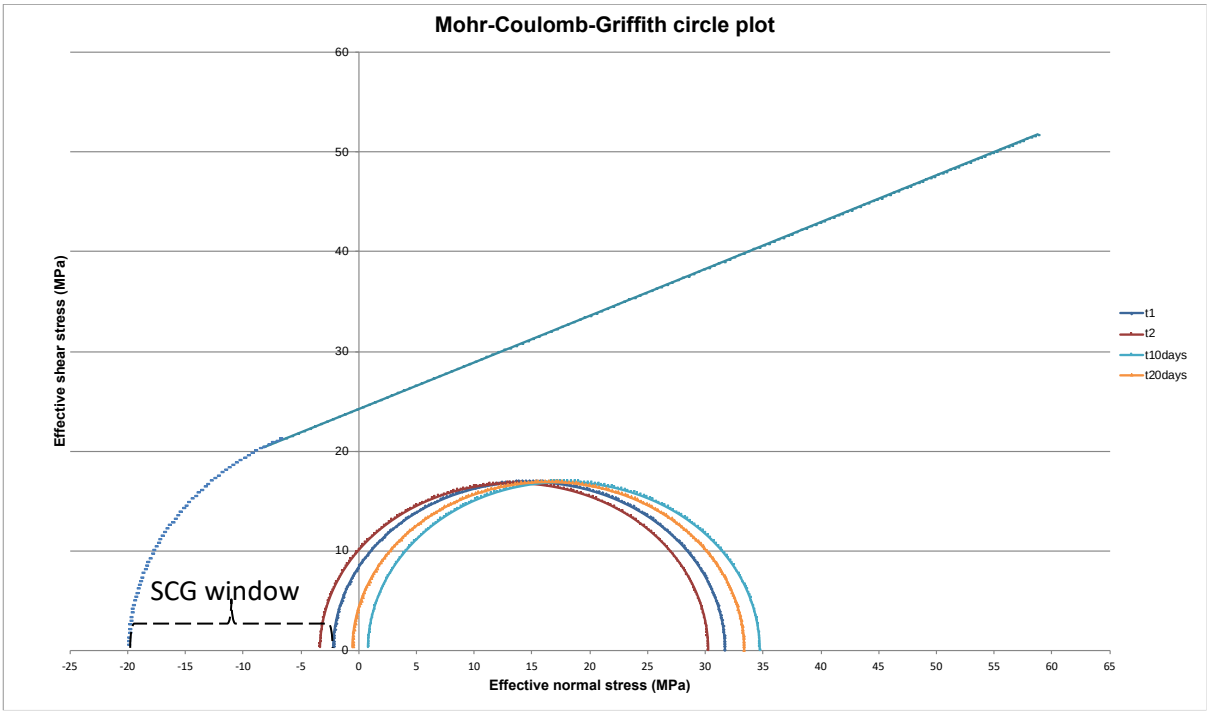

Figure 26: Mohr-Coulomb-Griffith envelope representing the evolution of effective stresses within a zone close to the injection source for case 3.

The third case presents σ_3' lower than 0 within 20 days after the beginning of the simulation (figure 26). After 2 months from the beginning of the simulation (t2), SCG conditions have been already met.

Figure 27:Mohr-Coulomb-Griffith envelope representing the evolution of effective stresses within a zone close to the injection source for case 4.

A value of K_I of 2 x 10^5 Pa*$m^{1/2}$ would correspond in crack growth velocity of 1.6 x 10^{-9} m/s. In the last simulation (case 4) the test of a relatively high injection rate leads the model to quickly reach the conventional failure state in the zones close the injection source (figure 28).The zones presenting a K_I value of 1.9 MPa*$m^{1/2}$ after 10 days are already failing in conventional tensile mode, as the half circles are crossing the Griffith parabola. At this stage the simulation can be interpreted as a conventional hydraulic fracturing treatment, where fractures are stimulated by injecting fluid above fracture pressure. Although the injection rates are not as high as they are in conventional fracturing treatments, the low porosity and permeability of the modeled rock-mass cause pore pressure to rise very fast because the fluid is not capable to easily migrate through the reservoir.

7.Discussion and Further Research

In this study, I presented ways of implementing the time-dependent (subcritical) fracturing theory coupled with the effect of this process on enhancing reservoir permeability relative to the enhancement of permeability. Additionally, I modeled pore pressure and stress state for different injection/production rates to determine conditions that may be favorable for SCG in conventional geothermal doublet systems. FLAC3D takes advantage of a continuum approach to represent the model domain. Numerical modeling has been chosen because of the ability to simulate large time and spatial scale processes within a reasonable time, by integrating existing geomechanical codes with data developed by previous studies.
Parameters like permeability and porosity are critical parameters to determine the feasibility of a geothermal project. Especially in deeper and hotter reservoirs, they can be very low, making the geothermal fluid hard to be naturally exploited. Despite their efficiency, conventional stimulation treatments are not always acceptable, because of the risks and hazards that can be associated with it (King, 2012).

The subcritical crack propagation has advantages compared to conventional fracturing treatment as it requires lower pressures (below fracturing pressure)(Lu et al., 2015; Waifo, 2010). Increase in fracture length or development of a fracture network may occur more gradual over time. Accordingly , this process does not require high injection pressures to enhance reservoir permeability as is the case for conventional hydraulic fracturing(Clark, 1949). Consequently, the risk of induced seismicity caused by fluid injections could be reduced(Porter et al., 2018). Moreover, more gradual fracture development may also limit risks of migration of fluid towards the surface, which wouldn't implicate contamination of shallower aquifers(Vengosh et al., 2014). SCG propagation is a very slow process. However, if time allowed to the crack for growing is sufficient, the crack growth rate can significantly increase. This observation has been confirmed by the model results, where crack growth rates significantly increase even if the change in net pressure is not dramatic. Furthermore, being such a slow process working at crack scale, a pressure drop after the initiation is less extreme, and the propagation can last long even at low constant injection rates. Effect of the subcritical crack growth on permeability changes have been explored. Results show that in a small model, average zone permeability increase up to 5 mD can be achieved with extremely low rates of injection.

In a geothermal doublet system, the conditions to promote subcritical crack propagation have been observed to be achievable in a reasonable amount of time comparing to the lifetime of a geothermal doublet. Under the conditions investigated, the initiation time was observed to be dependent on the injection rates. Lower injection rates resulted in larger amount of time before SCG initiation compared to higher rates of fluid injection. However, different petrophysical parameters will also play a major role.

Stress field required for SCG initiation resulted to be below the conditions to induce conventional failure. However, the in situ conditions will determine whether a system is far away or not from the failure point, which consequently will affect the injection rates necessaries to reach the SCG conditions. Slow crack velocity and limited effect on permeability have been observed especially in the first stages of the SCG regime. It remains a question whether the process is efficient enough to be used to stimulate reservoir permeability in real cases.

The current approach used in the lab-scale model, where crack growth mechanics and permeability enhancement are included, should be further implemented to a fully coupled extent, to completely capture the nature of the fracture propagation. Such model may be applied in the future at reservoir scale, to produce quantitative results about hydraulic conductivity changes for geothermal production purposes. Because geothermal reservoirs are associated with high temperature in situ, the effect of cold injections could lead to a thermoelastic response of the rocks around the injection well (T.K Perkins e al., 1985). Because this effect could considerably affect the injectivity, it needs to be incorporated in the numerical simulation. According to Zhurkov (1984), tensile strength in materials decreases over time. Subcritical propagation of cracks could further contribute to weaken the rock and tensile failure could occur in the rocks even at relatively low pressures. For this reason, a code taking into account the weakening of the rock over time and the occurrence of conventional tensile failure once KI_c has been exceeded, needs to be implemented.

To test the validity of my model, laboratory experiments may be performed in the near future using core samples from the Trias Westland geothermal reservoirs. Additionally, these experiments could be useful to better constrain the subcritical crack growth parameters, which could be then used in my model to simulate the time-dependent fracture behavior for a specific type of rock.

8.Conclusion

The numerical simulations carried out in FLAC3D resulted in a first attempt to explore the effect of subcritical growth of fractures to enhance reservoir permeability. Subcritical crack growth occurs for values of pressure lower than required for instantaneous breakage of the rock. Despite the simplicity of the models, time dependent (subcritical) fracturing results to affect permeability over time. Furthermore, within the SCG regime, the crack growth rate results to be time-dependent with the crack length increasing over time even at low constant injection rates. The conditions required for initiating SCG have been analyzed and the time of initiation of crack propagation resulted to be clearly dependent on the injection rates as well as the petrophysical parameters of the target rock.

Permeability is a crucial parameter within the exploration for geothermal purpose. Many reservoirs are estimated to be too tight and not economically valuable for geothermal production. Because of the risks associated with conventional stimulation treatments, stimulation jobs for geothermal purposes in the Netherlands are overall in standby and none have been performed recently. The validity of this theory could considerably contribute to increase the number of accessible reservoirs and potentially help the Netherlands to fast increase the amount of clean energy produced by geothermal fluid extraction.

Potential laboratory experiments on the application of this theory to core samples from tight geothermal reservoirs will give a better quantitative analysis on the timing of this process, also according to the petrophysical parameters variation within the sample.

References

- **Abdelmoneim SS, Nasr-EL-Din HA (2015) Determining the optimum HF concentration for stimulation of high temperature sandstone formations**. Society of Petroleum Engineers, SPE 174203-MS.
- **Atkinson B K, Subcritical crack propagation in rocks: theory, experimental results and applications**, Journal of structural geology, vol.4 1982**.**
- **Atkinson B K, 1984. Subcritical crack growth in geological materials.** J. Geophysics. Res., 89: p. 4077-4114.
- **Atkinson B K, Meredith P G, 1987. The theory of subcritical crack growth with applications to minerals and rocks. In: Atkinson (1987) Fracture Mechanics of Rock.** Academic press, London, p.111-162, p. 477-526.
- **A. Mignan, M. Broccardo, S. Wiemer, D. Giardini, Induced seismicity closed-form traffic light system for actuarial decision-making during deep fluid injections**, scientific reports 7, Article number: 13607(2017).
- **A. Vengosh, R. B. Jackson, N. Warner, T. H. Darrah, A. Kondash, A Critical Review of the Risks to Water Resources from Unconventional Shale Gas Developments and Hydraulic Fracturing in the United States**, Environment Science Technology, 2014, 48 (15), pp 8334-8348.
- **Britt, L.K., Smith, M.B., Haddad, Z., Lawrence, P., Chipperfield, S., Hellmann, T., 2006. Water-fracs: we do need proppant after all.** SPE 102227.
- **Bieniawski Z T, 1967. Mechanics of brittle fracture of rock.** Part I, II and III. Int. J. Rock Mech. Min. Sci. Vol. 4, 3 p. 95-430.
- **Charles R J, 1958. Static fatigue of glass.** J. Appl. Phys., 1958 (29): p. 1549-1560.
- **Charlez, P., Lemonnier, P., Ruffet, C., Boutéca, M.J., 1996. Thermally induced fracturing: analysis of a Field Case in North Sea.** In: Paper SPE 36916 Presented at EUROPEC, Milan, Italy, October 22–24, 8 pp.
- **Clark J.B., A hydraulic process for increasing the productivity of Wells,** Society of Petroleum Engineers, January 1949.
- **Coronado, J.A., 2007. Success of hybrid fracs in the basin.** SPE 106758.
- **Dake , L.P., 1978. Fundamentals of Reservoir Engineering**. Elsevier, Amsterdam.
- **Economides, M.J., Nolte, K.G., 1989, Reservoir Stimulation,** 2nd ed. Prenitce Hall, Upper Saddle river, NY, USA, 440 pp.
- **Economides, M.J., Nolte, K.G., 2000, Reservoir Stimulation,** 3rd ed. Wiley and Sons Ltd., United Kingdom.
- **Felder M., S. Fernandez, Core Hot shot NLW-GT-01, Panterra Geoconsultants,** February 2018.
- **Fredd, C.N., McConnell, S.B., Boney, C.L., England, K.W., 2000. Experimental study of hydraulic fracture conductivity demonstrates the benefits of using proppants.** SPE 60326.
- **Halliburton (2000a) Carbonate matrix acidizing treatment. Best practice series.** Halliburton, Houston.
- **International Energy Agency, Technology Roadmap: Geothermal Heat and Power.** May 2011.
- **Itasca.2018. FLAC3D 6.0 Manual.**
- **Irwin, G.R.: "Analysis of Stresses and Strains Near the End of a Crack Traversing a Plate,"** *Journal of Applied Mechanics* (September 1957) 24, 361–364.
- **Kear, J. and A.P. Bunger, 2014: "Dependence of static fatigue tests on experimental configuration for a crystalline rock".** Advanced Materials Research, 891: 863–871.
- **Ko, T. Y., Subcritical crack growth under mode I, II and III loading for Coconino sandstone,** The university of Arizona, 2008.
- **King, G. E. (2012. Hydraulic Fracturing 101: What every representative, environmentalist, regulator, reporter, investor, university researcher, neighbor and engineer should know about estimating frac risk and improving frac performance in unconventional gas and oil wells,** Society of Petroleum Engineers, SPE 152596.

- **Kirkman R., C. F. Arson, L. Stewart, R. Harris, A. Francis, The risks of hydraulic fracturing and the responsibilities for engineers.** Elem Sci Anth, 5, p.17. 2017
- **Lu, G., Uwaifo, E. C., Ames, B. C., Ufondu, A., Bunger, A.P., Prioul, R., Aidagulov, G. Experimental Demonstration of Delayed Initiation of Hydraulic Fractures below Breakdown Pressure in Granite,** ARMA 15-190.
- **Malate R.C.M. , J.J.C. Austria, Z.F. Sarmiento, G. Di Lullo, P.A. Sookprasong and E.S.Francia, Matrix stimulation treatment of geothermal wells using sandstone acid,** Standford University, Stanford, California, January 26-28, 1998.
- **Mayerhofer, M.J.,Meehan,D.N.,1998.Waterfracs—results from50cottonvalley wells.** SPE49104.
- **Perkins T.K, J.A. Gonzales, the effect of Thermoelastic stresses on Injection Well Fracturing,** Society of Petroleum engineers, 1985.
- **Portier S., L. André, Review on chemical stimulation techniques in oil industry and application to geothermal system,** January 2007.
- **Portier S., F.D. Vuataz, P. Nami, B. Sanjuan, A. Gerard, Chemical stimulation techniques for geothermal wells: experiments on the three-well EGS system at Soultz-sous-Forets, France,** Geothermics 38 (2009) 349-359.
- **Rafaela Marfil, Micheal Scherer, Maria Jesus Turrero, Diagenetic processes influencing porosity in sandstones from the Triassic Buntsanstein of the Iberian Range, Spain,** Sedimentary Geology 105 (1996) 203-219.
- **Reinicke A., E. Rybacki, S. Stanchits, E. Huenges, G. Dresen, Hydraulic fracturing stimulation techinques and formation damage mechanism – implications from laboratory testing of tight sandstone-proppant system,** Chemie der Erde 70 (2010) S3, 107-117.
- **Rushing, J.A., Sullivan, R.B., 2003. Evaluation of hybrid water-frac stimulation technology in the bossier tight gas sand play.** SPE 84394.
- **Senseny P.E, T.W.Pfeifle, Fracture Toughness of Sandstone and Shales**, American Rock Mechanics Association, 1984.
- **Shafiq M.U., H.B. Mahmud, Sandstone matrix acidizing knowledge and future development, J** Petrol Explor Prod Technol (2017) 7:1205-1216.
- **Sharma, M.M., Gadde, P.B., Sullivan, R., Sigal, R., Fielder, R., Copeland, D., Griffin, L., Weijers, L., 2004. Slick water and hybrid fracs in the bossier: some lessons learnt.** In: Paper SPE 89876 Presented at the SPE Annual Technical Conference and Exhibition, Houston, TX, USA, September 26–29, 12 pp.
- **Schultz R., G. Atkinson, D. W. Eaton, Y. J. Gu, J. Kao, Hydraulic fracturing volume is associated with induced earthquake productivity in the Dauvernay play.** Science 19 Jan 2018, Vol. 359, issue 6373,pp. 304-308.
- **Siratovich P.A., M.C. Villenueve, J.W. Cole, B.M. Kennedy, F. Begue, SWaturated heating and quenching of three crustal rocks and implications for stimulation of permeability in geothermal reservoirs.** International Journal of Rock Mechanics & Mining Sciences 80 (2015) 265-280.
- **http://www.shale-gas-information-platform.org/areas/basics-of-shale-gas/induced-seismicity.html**
- **Smith CF, Hendrickson AR (1965) Improved success in acid stimulation with a new organic-HF system**. Society of Petroleum Engineers, SPE-36907-MS.
- **TNO 2014 R11396 | DoubletClac 1.4 manual English version for DoubletCalc 1.4.3.**
- **TNO 2015 R11618|Final report. Sector Outlook: Geothermal power increase in the Netherlands by enhancing the capacity.**
- **Uwaifo Efosa Christopher, Time-dependent initiation of multiple hydraulic fractures in rocks,** University of Pittsburgh, 2015.
- **Warpinski, N.R., 2009. Stress amplification and arch dimension in proppant beds deposited by waterfracs**. SPE 119350.
- **William L. Ellsworth, Injection-Induced Earthquakes,** Science, VOL 341, 12 July 2013.
- **www.ta.survey.nl , Trias Westland Geothermal energy project.**
- **Zhurkov S.N.. Kinetic concept of the strength of solids.** International Journal of Fracture 26 (1984) 295-307.